bif1, a new BMP signaling inhibitor, regulates embryonic hematopoiesis in the zebrafish

Ghersi, Joey Jimmy; Mahony, Christopher; Bertrand, Julien

© 2019. Published by The Company of Biologists Ltd | Development (2019) 146, dev164103. doi:10.1242/dev.164103

RESEARCH ARTICLE

bif1, a new BMP signaling inhibitor, regulates embryonic hematopoiesis in the zebrafish

Joey J. Ghersi, Christopher B. Mahony and Julien Y. Bertrand*

ABSTRACT

Hematopoiesis maintains the entire blood system, and dysregulation of this process can lead to malignancies (leukemia), immunodeficiencies or red blood cell diseases (anemia, polycythemia vera). We took advantage of the zebrafish model that shares most of the genetic program involved in hematopoiesis with mammals to characterize a new gene of unknown function, *si:ch73-299h12.2*, which is expressed in the erythroid lineage during primitive, definitive and adult hematopoiesis. This gene, required during primitive and definitive erythropoiesis, encodes a C2H2 zinc-finger protein that inhibits BMP signaling. We therefore named this gene blood-inducing factor 1 and BMP inhibitory factor 1 (*bif1*). We identified a *bif1* ortholog in *Sinocyclocheilus rhinocerous*, another fish, and in the mouse genome. Both genes also inhibit BMP signaling when overexpressed in zebrafish. In conclusion, we have deorphanized a new zebrafish gene of unknown function: *bif1* codes for a zinc-finger protein that inhibits BMP signaling and also regulates primitive erythropoiesis and definitive hematopoiesis.

KEY WORDS: Zebrafish, Erythropoiesis, Definitive hematopoiesis, Hematopoietic stem cells, BMP signaling, Zinc finger proteins

INTRODUCTION

Red blood cells (RBCs) constitute the majority of the circulating blood cells and play a major role in the transport of respiratory gases. They are constantly replenished through a process called erythropoiesis, and are derived from hematopoietic stem and progenitor cells (HSPCs) in adults. The molecular basis of this process has been largely elucidated through the use of different *in vivo* models, such as *Xenopus*, zebrafish and mice, and *in vitro* models, such as human umbilical cord blood differentiation (Nandakumar et al., 2016) or the study of embryonic stem cell differentiation. In all vertebrates, the production of RBCs occurs in two major waves during development: primitive and definitive erythropoiesis (Palis, 2014). Both processes lead to the formation of RBCs with molecular differences such as the expression of different hemoglobin genes (Sankaran and Orkin, 2013).

In the zebrafish embryo, multiple waves of hematopoiesis give rise to distinct waves of erythropoiesis. During primitive erythropoiesis, *gata1*, a master regulator of erythropoiesis, is expressed in the posterior lateral plate mesoderm (PLPM) as early as 12 h post fertilization (hpf) (Detrich et al., 1995; Long et al., 1997). At 18 hpf, after PLPM stripes have converged to the midline, erythroid progenitors differentiate and proliferate in the intermediate cell mass (ICM) (Al-Adhami Ma, 1977). This primitive erythropoiesis is similar to what is observed in mammals, where primitive RBCs arise in the yolk sac directly from mesodermal progenitors (Palis et al., 1999; Keller et al., 1999). As definitive hematopoiesis arises, a transient wave of erythro-myeloid progenitors (EMPs) appears in the posterior blood island of the zebrafish embryo. Although the contribution of these progenitors is hard to quantify *in vivo*, we have previously shown that they could differentiate into erythroid cells *in vitro* (Bertrand et al., 2007). Mouse EMPs develop in the yolk sac and give rise to a clearly identified RBC population that expresses specific hemoglobins (McGrath et al., 2011). Finally, HSPCs emerge in the ventral floor of the dorsal aorta in zebrafish (Bertrand et al., 2010), similar to the aorta-gonad-mesonephros in mammals (Medvinsky and Dzierzak, 1996). HSPCs migrate to the caudal hematopoietic tissue (CHT), where they expand and differentiate into all major hematopoietic lineages (Murayama et al., 2006). Although the cell and non-cell autonomous signals that govern RBC production from definitive hematopoietic progenitors are well characterized, the signals that specify mesoderm into primitive RBCs are still largely unknown. *gata1*, as well as *lmo2* and *scl/tal1* can be detected as early as 12 hpf in the PLPM during zebrafish development (Thompson et al., 1998; Liao et al., 1998; Detrich et al., 1995). However, the signals that control the expression of these genes, and hence the commitment of mesoderm progenitors towards the erythroid lineage, are still poorly understood.

Bone morphogenetic proteins (BMPs) are members of the TGF-β family and are central players in the BMP signaling pathway, which is involved in several processes, such as cancer, bone formation and mesoderm specification (Zhang et al., 2016; Wu et al., 2016; Chen et al., 2004). During gastrulation, high BMP activity specifies the ventral part of the embryo, while BMP inhibitors are expressed dorsally (Pomreinke et al., 2017). At this stage, high BMP activity specifies mesodermal cells into blood lineage, as shown by severe hematopoietic defects in *bmp4*- and *smad5*-deficient mouse embryos (Winnier et al., 1995; Liu et al., 2003). For example, *bmp4* mutant mouse embryos die early during embryogenesis, but the few embryos that survive show a strong reduction in primitive erythropoiesis (Winnier et al., 1995). Upon the binding of BMP ligands to their receptors, R-smads (*smad1*, *smad5* and *smad9* in zebrafish) are phosphorylated. Activated R-smads bind the co-smad *smad4* and translocate to the nucleus to activate the transcription of target genes by binding to BMP-responsive elements (BRE) (Katagiri et al., 2002). To date, several genetic screens have identified many zebrafish mutants with mutations in components of the BMP signaling pathway, such as *bmp2b*, *bmp7* or *smad5* (Kishimoto et al., 1997; Hild et al., 1999; Schmid et al., 2000). These mutants share a common dorsalized phenotype due to a problem in dorso-ventral patterning during gastrulation (Kondo, 2007). This signaling pathway is tightly regulated during development at the cell- and non-cell-autonomous level. At the

University of Geneva, School of Medicine, Department of Pathology and Immunology, CMU, University of Geneva, CH-1211 Geneva 4, Switzerland.

*Author for correspondence (julien.bertrand@unige.ch)

J.Y.B., 0000-0001-6570-4082

Received 6 February 2018; Accepted 22 February 2019

Development (2019) 146, dev164103. doi:10.1242/dev.164103

non-cell-autonomous level, *chordin* and *noggin* are the major secreted inhibitors against BMP signaling, and are expressed in the organizer during gastrulation (Fürthauer et al., 1999; Smith and Harland, 1992; Sasai et al., 1994). Mutants for *chordin* (*chordino*) show a strong ventralization phenotype owing to the change in dorso-ventral BMP gradient (Hammerschmidt et al., 1996). At the cell-autonomous level, the inhibitory Smads (*smad6* and *smad7*) inhibit the binding of R-smads to the BMP receptors, to the co-smad and to DNA, leading to an inhibitory effect on BMP activity. *Smad7* was found to increase the self-renewal of HSPCs and to promote myeloid differentiation in human and murine systems, respectively (Chadwick et al., 2005; Blank et al., 2006). *SMAD6*, by interfering with *SMAD5* and *SMAD4*, inhibits erythropoiesis from human umbilical cord blood progenitors (Kang et al., 2012).

Here, we have elucidated the role of an uncharacterized gene, *si:ch73-299h12.2*, that was primarily described as highly enriched in endothelial and hematopoietic cells sorted from 26-28 hpf *Tg(fli1a:egfp)* zebrafish embryos (Cannon et al., 2013). This gene of unknown function encodes a C2H2 zinc-finger protein, the expression of which progressively becomes restricted to the primitive erythroid lineage during early development, and is maintained in definitive hematopoietic progenitors. We named this gene *bif1*, as our results show that this new gene is important for the development of erythropoiesis (blood-inducing-factor 1) and that it does so by inhibiting the BMP pathway (BMP-inhibitory-factor 1).

RESULTS

si:ch73-299h12.2 (*bif1*) encodes a C2H2 nuclear protein

bif1 is a gene of unknown function in a cluster of the telomeric region of chromosome 21. It has a simple structure consisting of two exons and one intron (Fig. 1A). *bif1* encodes a protein containing ten C2H2 zinc-finger motifs (Fig. 1A). These domains are known to bind DNA and act as transcription factors, but these motifs can also bind RNA or proteins (Brown, 2005; Brayer and Segal, 2008; Wolfe et al., 2000). The prediction site also indicates a classical bipartite nuclear localization site (NLS) in Bif1. To test the ability of Bif1 to

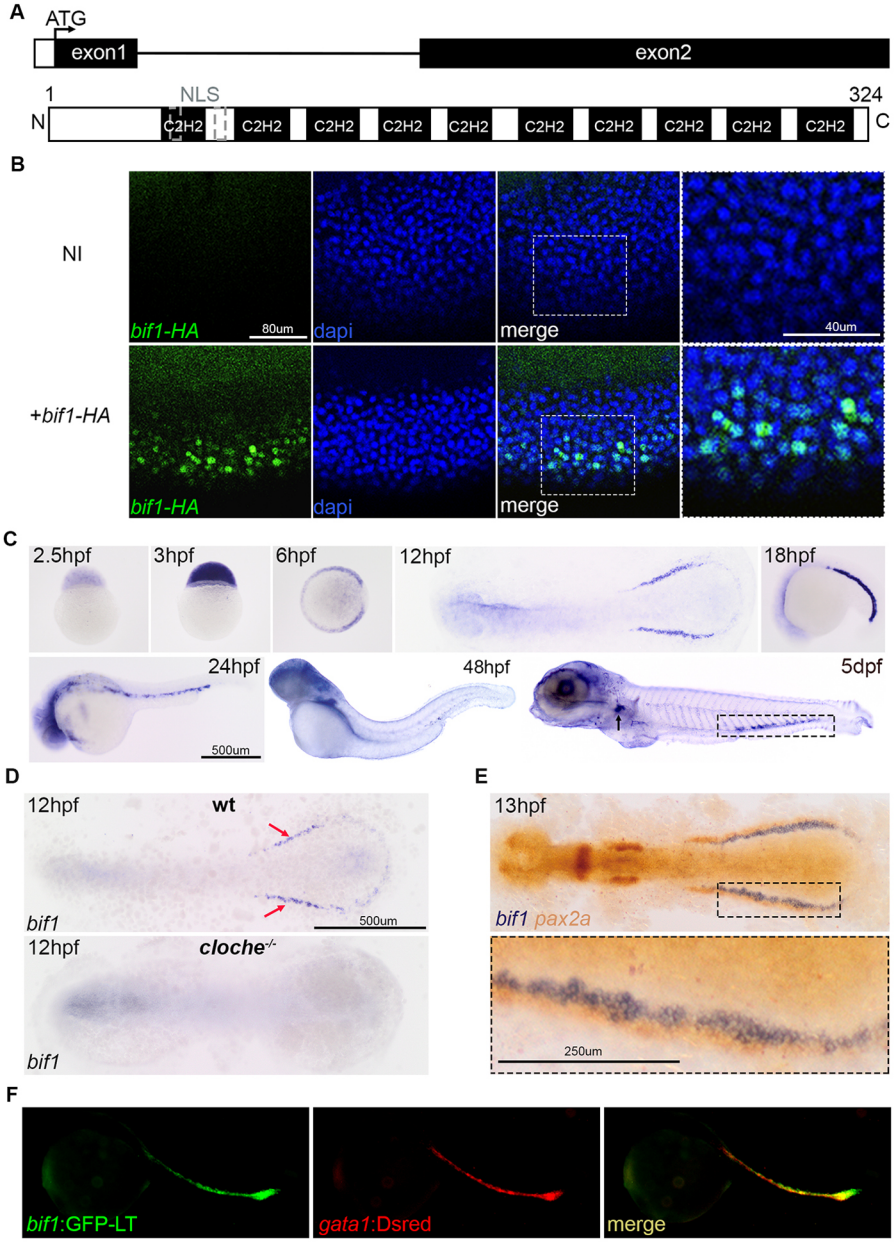

Fig. 1. Bif1, a C2H2 zinc-finger protein, is expressed at an early stage and becomes restricted to the erythroid lineage during primitive erythropoiesis. (A) Representation of the *bif1* gene and protein structures. NLS, nuclear localization sequence. (B) Immunofluorescence using an antibody against HA and DAPI staining on 6 hpf non-injected embryos or embryos injected with *bif1-HA* mRNA. The area shown at higher magnification is indicated with a dotted rectangle. (C) Time-course expression of *bif1* revealed by whole-mount *in situ* hybridization. The arrow and the dotted rectangle represents the pronephric glomerulus and the caudal hematopoietic tissue, respectively. (D) Expression of *bif1* at 12 hpf in wild type and a *cloche* mutant. The red arrows show the expression of *bif1* that is lost in the *cloche* mutant. (E) Double whole-mount *in situ* hybridization against *bif1* (blue) and *pax2* (orange, representing the intermediate mesoderm) at 13 hpf embryos. The area shown at higher magnification is indicated with a dotted rectangle. (F) Images of 23 hpf fluorescent fish carrying two constructs: *Tg(bif1:GFP-LT)* and *Tg(gata1:DsRed)*.

Development (2019) 146, dev164103. doi:10.1242/dev.164103

translocate to the nucleus, we cloned a mRNA coding for a HA-tagged Bif1. This *bif1-HA* mRNA was injected into wild-type embryos, and we performed anti-HA immunofluorescence at 6 hpf. In injected embryos, we observed staining in the nucleus (Fig. 1B). Therefore, Bif1 is able to translocate to the nucleus, and could potentially bind DNA to act as a transcription factor.

bif1 is progressively restricted to the erythroid compartment during embryogenesis

During embryogenesis, the maternal-to-zygotic transition occurs around 2.5 hpf (Tadros and Lipshitz, 2009). As *bif1* starts to be expressed at 3 hpf, it is likely a zygotic mRNA (Fig. 1C). At 6 hpf, *bif1* is expressed in the margin and in the animal pole of the embryo following a dorso-ventral gradient, but no expression was seen in the dorsal organizer (Fig. 1C). From 12 hpf to 6 days post fertilization (dpf), *bif1* expression is highly similar to that of *gata1*: it is first expressed in the PLPM at 12 hpf, then its expression becomes specific to the ICM at 18 hpf, before it is expressed in circulating erythroblasts at 24 hpf (Fig. 1C). It is then expressed in the CHT between 2 dpf and 5 dpf (Fig. 1C and Fig. S1). At this stage, *bif1* also starts to be detected in the glomerulus area, the ultimate site of hematopoiesis (Fig. S1). To confirm expression in the PLPM, we investigated the expression of *bif1* in *cloche* mutants, as well as its relationship to *pax2a*-expressing cells (intermediate mesoderm). We found that *bif1* was absent in *cloche* mutants, and that *bif1*-positive cells were juxtaposed to *pax2a*-positive cells (Fig. 1D,E). To confirm the erythroid expression, we generated double transgenic animals *Tg(bif1:GFP-LT;gata1:DsRed)*. Between 20 and 24 hpf, GFP-LT expression recapitulated the same pattern as observed by whole-mount *in situ* hybridization, and showed fluorescence in the ICM, overlapping with that of *Tg(gata1:DsRed)* in double transgenic embryos (Fig. 1F). Altogether, these data show that *bif1* becomes progressively restricted to the erythroid lineage as embryogenesis occurs.

bif1 is also expressed in definitive HSPCs and their lymphoid progeny

During definitive hematopoiesis, HSPCs are produced from the ventral floor of the dorsal aorta (VDA) (Bertrand et al., 2010; Kissa and Herbomel, 2010). In the double transgenic animals *Tg(bif1:GFP-LT;flk1:mCherry)*, we found double-positive cells in the VDA showing that *bif1* is expressed in HSPCs at 36 and 48 hpf (Fig. 2A,B). Later, we identified GFP-LT-positive cells in the CHT, indicating that *bif1* is still expressed in HSPCs when they expand in the CHT (Fig. 2C,D). Finally, in the thymus, where definitive lymphopoiesis occurs, we observed double-positive cells in double transgenic *Tg(bif1:GFP-LT;rag2:DsRed)* animals (Fig. 2E,F). Although *bif1* was never observed by whole-mount *in situ* hybridization in the thymus, the presence of these rare double-positive cells could be due to the long lifespan of GFP-LT expressed by HSPCs. Altogether, these results show that *bif1* is expressed during definitive hematopoiesis.

bif1 is maintained in erythroid precursors in the adult whole kidney marrow

We took advantage of the *Tg(gata1:DsRed)* transgenic line and sorted, after dissecting the whole kidney marrow (WKM), different hematopoietic cell populations based on scatter populations and levels of DsRed expression: the lymphoid/progenitor fraction was subdivided into lymphocytes (L/PNE – lymphoid/precursor gate non erythroid; *gata1:DsRed*$^{-}$), erythroid progenitors (*gata1:DsRed*^{low}) and mature RBCs (*gata1:DsRed*^{high}). Myeloid cells were used as control (Fig. 2G). By qPCR we found an enrichment of *bif1* in the two erythroid compartments (Fig. 2H). Therefore, *bif1* also marks the definitive erythroid lineage in the adult; however, we never observed this erythroid expression with our *bif1:GFP-LT* animals (data not shown).

bif1 regulates primitive and definitive erythropoiesis

In order to identify the function of this new gene during erythropoiesis, we overexpressed *bif1* and analyzed *gata1* expression at 12 hpf. About 50% of the embryos showed an ectopic expression of *gata1* in the posterior part of the PLPM (Fig. 3A). However, *flk1* or *acta2* were not altered, showing that *bif1* gain-of-function did not interfere with angioblasts or paraxial mesoderm (Fig. 3B). To assess the specific role of *bif1* in this phenotype, we also injected a mutated *bif1* mRNA (*bif1MUT*) resulting in a non-functional NLS. This mutated mRNA failed to induce ectopic *gata1* at 12 hpf (Fig. S2A,B). The erythroid and pronephric lineages are both derived from the same mesoderm territory. It has previously been shown that BMP signaling affects the balance between these two lineages (Gupta et al., 2006) and we wondered whether *bif1* also played a role here. By performing a double whole-mount *in situ* hybridization against *pax2a* and *gata1*, we observed an increase of *gata1* expression compared with *pax2a* in the embryos injected with *bif1* mRNA (Fig. 3C,D). This increase in *gata1* occurred at the expense of the *pax2a* territory (Fig. S3), suggesting that *bif1* affects the balance between the erythroid and pronephric lineages. As the expression of *bif1*, by *in situ* and in transgenic animals, always seems to correlate with early stages of erythroid differentiation, we speculated on a potential role for *bif1* in regulating early stages of erythropoiesis. After *bif1* mRNA injection, we collected blood samples from 4 dpf embryos and performed a May–Grünwald–Giemsa staining. Interestingly, in *bif1*-injected embryos, erythroid cells appeared bigger than in control embryos, therefore less differentiated, although the nucleus was condensed (Fig. 3E,F). Their morphology was still very different from adult erythrocytes (Fig. 3F). Altogether, we conclude that *bif1* alters/controls the terminal differentiation of erythroid progenitors.

As *bif1* affects primitive erythropoiesis, we wanted to know whether it could also affect definitive erythropoiesis. According to previous reports, definitive erythropoiesis is initiated in the CHT (Murayama et al., 2006) at around 4 dpf, when primitive erythrocytes are still present in the embryo (Willett et al., 1999). In order to specifically investigate the role of *bif1* in definitive erythropoiesis, we first ablated primitive RBCs, by treating embryos with phenylhydrazine (PHZ) (Shafizadeh et al., 2004). Control embryos treated with PHZ recover from the induced anemia 4 days after the drug is removed. To analyze the potential role of *bif1* during recovery, we generated a transgenic line in which *bif1* is expressed under the control of the heat shock-70 promoter (*hsp70l*). This construct allowed us to overexpress *bif1* every day, by heat-shocking the embryos (Fig. 3G). In order to measure the difference in recovery, we performed O-dianisidine staining at 4 dpf. In transgenic embryos, there was a better recovery of erythroid progenitors in the CHT at 4 dpf, based on hemoglobin content as measured by O-dianisidine (Fig. 3H,I). In normal conditions, without chemically induced anemia, we observed a slight increase of *gata1* expression but no differences in HSPC or neutrophil content in the CHT at 4 dpf (Fig. S4). Therefore, overexpression of *bif1* aids the recovery from a chemically induced anemia by increasing definitive erythroid progenitors in the CHT.

To complement our gain-of-function experiments, we knocked down *bif1* using a morpholino. We observed a strong decrease of

Development (2019) 146, dev164103. doi:10.1242/dev.164103

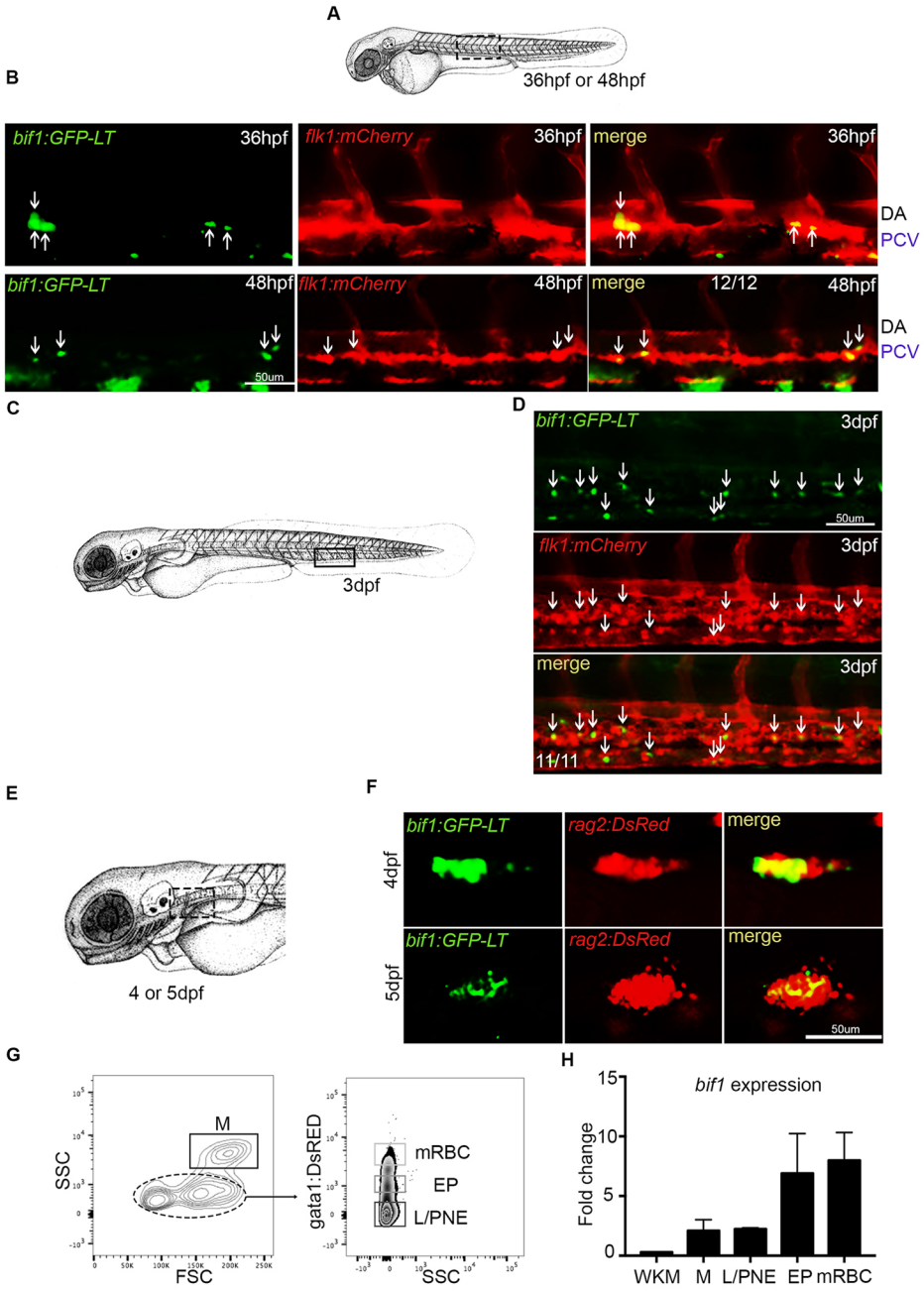

Fig. 2. *bif1* is also expressed during definitive and adult hematopoiesis. (A) Schematic indicating the approximate area in the trunk shown in the images in B (dotted rectangle). (B) Confocal images of the trunk region of double-positive *bif1*:*GFP-LT* and *flk1*:*mcherry* embryos at 36 hpf and 48 hpf. Arrows indicate double-positive cells. (C) Schematic indicating the approximate area in the tail shown in the images in D (rectangle). (D) Confocal images of the CHT of double-positive *bif1*:*GFP-LT* and *flk1*:*mcherry* embryos at 3 dpf. Arrows indicate double-positive cells. (E) Schematic representing the head of a zebrafish at 4 dpf. The position of the thymus is outlined by the dotted rectangle. (F) Confocal images of thymic area of double-positive *bif1:GFP-LT;rag2:DsRed* embryos at 4 and 5 dpf. (G) Results from FACS-sorted cells of WKM dissected from 1-year-old embryos. *n*=3. (H) Expression of *bif1* by qPCR on FACS-sorted cells, relative to the WKM. Data were obtained from biological triplicates. SSC, side scatter; FSC, forward scatter; M, myeloid; L/PNE, lymphocytes and progenitors non-erythroid; EP, erythroid progenitors; mRBC, mature red blood cells; WKM, whole kidney marrow.

circulating RBCs at 3 dpf (scored by O-dianisidine staining), which was rescued by the injection of *bif1* mRNA (Fig. 4A,B and Fig. S11A,B,C,E). This phenotype was quite specific, as we did not observe any change in primitive myelopoiesis or in the development of vasculature or somites when *bif1* was knocked down by a morpholino (Fig. S5A-C), thus confirming that *bif1* is necessary for erythropoiesis only during primitive hematopoiesis. In order to determine whether *bif1* was also required for erythroid progenitors in the CHT, we performed whole-mount *in situ* hybridization against *gata1* at 4 dpf. We observed a loss of *gata1* expression in the CHT (Fig. 4C), linked to an increase in cell death, as measured by Acridine Orange staining in *bif1* morphants (Fig. S6). However, this was not specific to the erythroid lineage, as *rag1* was lost at 5 dpf in the thymus (Fig. 4D) and *cmyb* was lost at 4 dpf in the CHT (Fig. 4E), showing a defect in definitive hematopoiesis. As we found that *bif1* is expressed in HSPCs during their specification in the VDA (Fig. 2B), we wondered whether the emergence of HSPCs was also altered in *bif1* morphants. Both *runx1* and *cmyb* were affected in *bif1* morphants, whereas *gata2b* was not (Fig. 4F). Altogether, these results point out the importance of *bif1* in definitive hematopoiesis, as well as in primitive erythropoiesis.

bif1 inhibits the BMP signaling pathway

As stated above, the balance between intermediate and lateral plate mesoderm is partially controlled by BMP signaling. Moreover, the ectopic expression of *gata1* at 12 hpf in the PLPM has already been described in BMP-deficient embryos, such as *bmp4* mutants (Stickney et al., 2007). Additionally, BMP-deficient embryos exhibit dorsalized morphologies, as well as defective cloaca development and the formation of ectopic tail structures (Pyati et al., 2006; Yang and Thorpe, 2011; Mullins et al., 1996). We could observe all these phenotypes in embryos injected with *bif1* mRNA

Development (2019) 146, dev164103. doi:10.1242/dev.164103

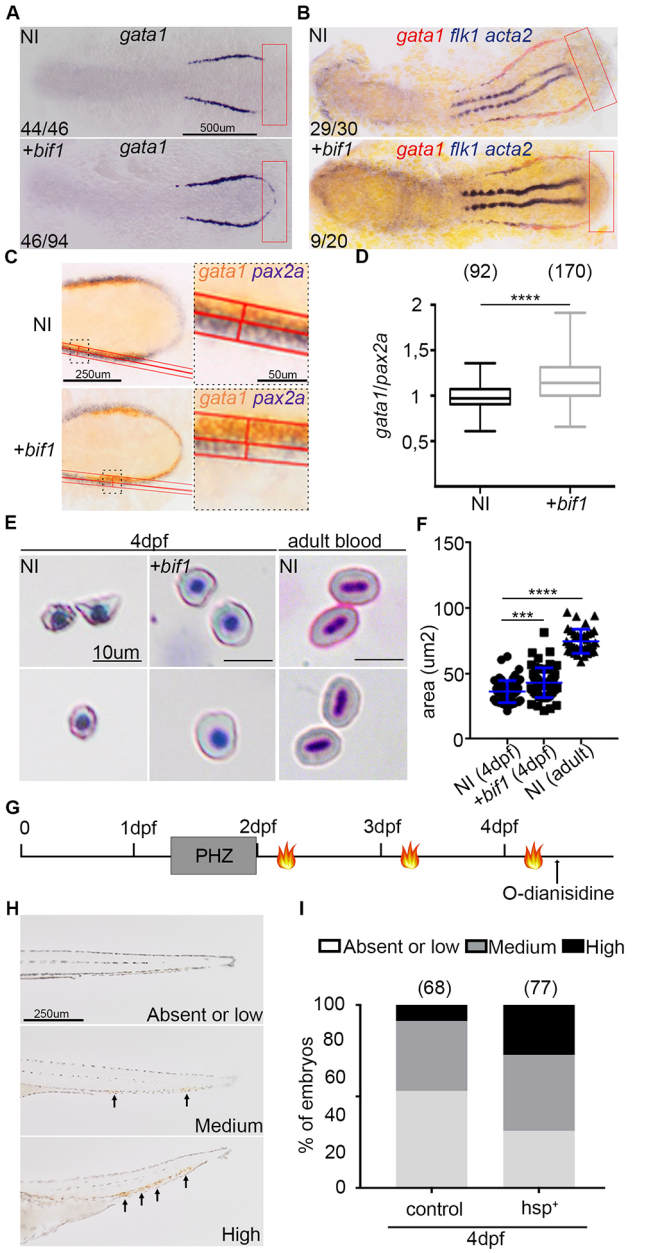

Fig. 3. *bif1* affects erythropoiesis. (A) Whole-mount *in situ* hybridization for *gata1* at 12 hpf in non-injected embryos or embryos injected with *bif1* mRNA. The red rectangle shows the ectopic region where *gata1* is expressed in *bif1*-injected embryos. (B) Double whole-mount *in situ* hybridization, at 14 hpf, for *gata1* (red) and *flk1* (blue), a marker of the first angioblasts. (C) Whole-mount *in situ* hybridization for *gata1* (orange) and *pax2a* (blue) in 12 hpf non-injected embryos or embryos injected with *bif1* mRNA. The areas shown at higher magnification are outlined with a dotted rectangle. The red line defines the width of expression for these two stainings. (D) For each embryo, we measured the ratio of *gata1* and *pax2a* width. The lowest and highest points of the whiskers indicate the extreme values. The boxes indicate the 25-75th percentile range. (E) May–Grünwald–Giemsa staining of circulating RBCs, from non-injected embryos or embryos injected with *bif1* mRNA at 4 dpf and 6 months, after a cytospin. (F) RBC diameters. The symbols indicate individual data points. (G) Experimental outline of the PHZ-induced anemia followed by three heat shocks at 38°C for 45 min (flames). (H) Bright-field images of tails, indicating the different levels of O-dianisidine staining (arrows). (I) Percentage of embryos showing absent or low (light gray), medium (dark gray) or high (black) levels of hemoglobin, as shown by O-dianisidine staining. Statistical analysis was carried out using an unpaired Student's *t*-test. Data are mean±s.e.m. ****P<0.0001.

(Fig. 5A,B and Fig. S7A,B). Again, this dorsalizing phenotype was specific as it was strongly reduced when the NLS in *bif1* was mutated (Fig. S2C,D). Similarly, we overexpressed *si:ch73-299h12.3* mRNA, a close paralog of *bif1* sharing more than 58% similarity at the protein level (Fig. S8A) with an expression pattern that is highly similar to *bif1* (Fig. S8B). This highly similar paralog did not induce dorsalization, but rather cyclopia (Fig. S8C), and did not affect *gata1* in the way *bif1* mRNA did (Fig. S8D). This suggests that the phenotypes observed in *bif1* gain of function were *bif1* specific. This strong dorsalizing phenotype did not seem to impair primitive myelopoiesis (Fig. S5D), and vasculogenesis was difficult to assess due to the overall morphology of the embryos (Fig. S5E). From these results, we therefore hypothesized that *bif1* inhibits the BMP signaling pathway. In order to confirm our hypothesis, we analyzed the level of BMP signaling by measuring the levels of phosphorylated Smad1, Smad5 and Smad9, as these proteins are specifically phosphorylated in response to BMP ligands. *bif1* gain of function caused a decrease in the ratio of p-Smad/Smad, therefore arguing in favor of an inhibition of the BMP signaling pathway (Fig. 5C,D). Moreover, in the *Tg(BRE:eGFP)* reporter line, where eGFP is expressed under the control of BMP responsive elements, *bif1* decreased the number of eGFP^{+} cells (Fig. 5E), as well as their mean fluorescence intensity (data not shown), showing a strong decrease in BMP activity *in vivo*. The dorsalization induced by *bif1* was rescued through co-injection of *bmp2b* mRNA, one of the BMP ligands (Fig. 5B), which by itself led to ventralization (Fig. S9). In *bif1* morphants, we found a systematic reduction in eye size (Fig. 5F,G) which was not due to developmental delays, according to the size of otoliths (Fig. S10A, B). This phenotype is known to be linked with a higher level of BMP activity (Song et al., 2013), as scored by higher levels of p-Smad1, Smad5 and Smad9 (Fig. 5H). This phenotype was rescued by the injection of *bif1* mRNA (Fig. S11D). Altogether, these results point to *bif1* as a new endogenous inhibitor of the BMP signaling pathway. In order to precisely elucidate the molecular function of *bif1*, we analyzed, using whole-mount *in situ* hybridization, the expression of genes known to play a role in BMP signaling. At 6 hpf, *bmp4* and *bmp2b* were decreased after *bif1* overexpression, whereas the other members tested were not affected (Fig. S12A,B). Further analyses will be required to fully understand the precise molecular function of *bif1*. Finally, we looked at a potential feedback loop from BMP signaling over *bif1* expression. We found an increase and a decrease of *bif1* expression when we injected *smad6a* and *bmp2b*, respectively (Fig. 5I,J). These results show that the BMP pathway negatively regulates *bif1* expression. During gastrulation, BMP signaling and *bif1* inhibit each other, which probably contributes to fine-tuning the dorsoventral gradient of BMP signaling. Finally, we sought to investigate whether *bif1* could mediate its effect on erythropoiesis by inhibiting the BMP signaling pathway. Therefore, we analyzed the morphology of RBCs after *smad6a* mRNA overexpression to inhibit the BMP pathway. After examining RBC morphology, we obtained a similar result to that obtained after *bif1* overexpression (Fig. S13). Therefore, we conclude that *bif1* regulates erythropoiesis through its ability to inhibit the BMP pathway.

bif1 is present in other phyla

We investigated the presence of *bif1* orthologs in other species. In order to find a potential ortholog, we blasted the protein sequence of *bif1* against known proteomes (blast.ncbi.nlm.nih.gov/) and identified more than 30 zebrafish proteins due to the highly conserved C2H2 sequences (data not shown). Moreover, we also

Development (2019) 146, dev164103. doi:10.1242/dev.164103

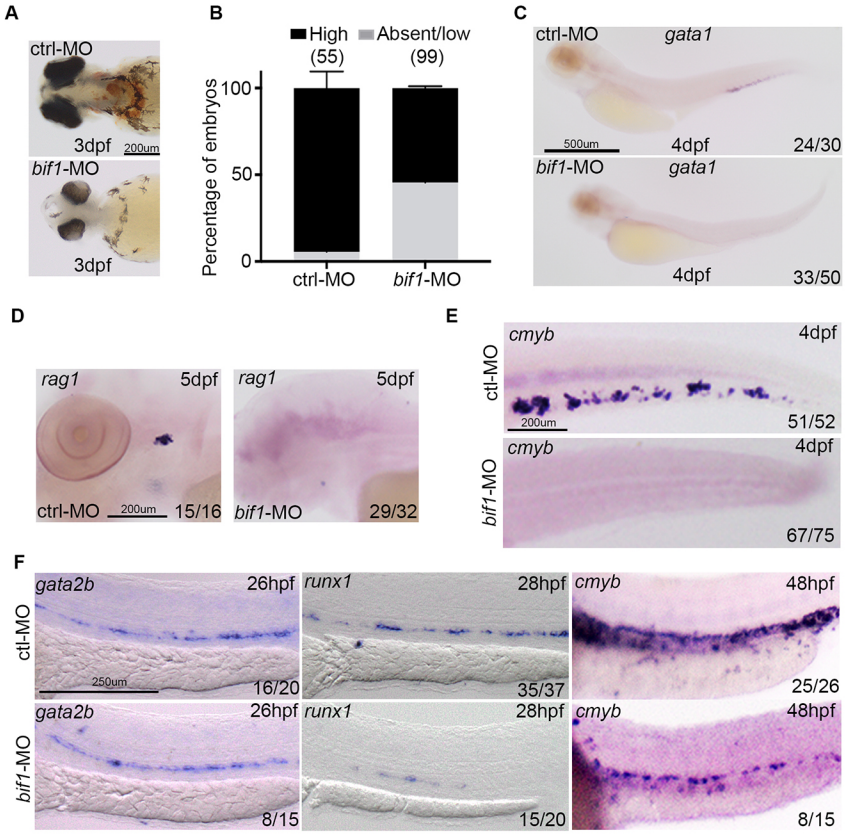

Fig. 4. *bif1* affects definitive hematopoiesis. (A) Bright-field images from O-dianisidine-stained embryos at 3 dpf. These embryos are injected with a control morpholino or a morpholino against *bif1*. (B) Percentage of embryos showing absent/low (gray) or high (black) levels of hemoglobin. Data are mean±s.e.m. (C-F) Whole-mount *in situ* hybridization for *gata1* at 4 dpf (C), *rag1* at 5 dpf (D), *cmyb* at 4 dpf (E), *gata2b* at 26 hpf, *runx1* at 28 hpf and *cmyb* at 48 hpf (F), in embryos injected with control morpholino (ctrl-MO) or morpholino against *bif1* (*bif1*-MO).

found a potential ortholog in *Sinocyclocheilus rhinocerous* (*S. rhino*) – *LOC107737464* – that shares 57.8% of similarity at the protein level (Fig. S14). Although zebrafish and *S. rhino* do not belong to the same subfamily order, they are both cyprinids. Both species share a similar genome organization near these two genes, as observed by synteny analysis (Fig. 6A). We injected the full-length mRNA for *S. rhino LOC107737464* into zebrafish embryos. At 24 hpf, these embryos were dorsalized, although to a lesser extent than the dorsalization produced by *bif1* overexpression (Fig. 6B), demonstrating that *S. rhino bif1* can also inhibit BMP signaling in the zebrafish embryo. However, no significant alteration in *gata1* expression was observed in embryos overexpressing this potential ortholog of *bif1* (Fig. 6C). We wondered whether *bif1* was also present in mammals. We blasted each Bif1 protein sequence from these two fish species against the *Mus musculus* protein database and identified one potential ortholog. *Zfp944* shows 39.1% similarity to *Danio rerio* Bif1 at the protein level (Fig. S15A). Moreover, this gene seems to be expressed at low levels in erythroid cells during primitive, fetal and adult erythropoiesis, according to the Erythron database (www.cbil.upenn.edu/ErythronDB/). This gene is present on chromosome 17, in a cluster of genes encoding zinc-finger proteins, a situation that is reminiscent of the cluster where *bif1* lays in the zebrafish genome. When we injected the full-length *Zfp944* mRNA into one-cell stage zebrafish embryos, we observed a dose-dependent dorsalization (Fig. 6D,E), correlated to a decrease of BMP signaling activity, as observed in *Tg(BRE:eGFP)* (Fig. S15B). However, no effect was found on *gata1* expression at 12 hpf, similar to *S. rhino bif1* (Fig. 6F), but at 48 hpf, the overexpression of the three transcripts induced a similar decrease of *gata1*, as measured by qPCR on whole embryos (Fig. 6G), which might explain the abnormal erythroid differentiation observed at 4 dpf (Fig. 3E,F). Altogether, we found that *Zfp944* in *M. musculus* is also able to inhibit BMP signaling in zebrafish embryo. However, additional experiments will be required to address its potential role during mouse erythropoiesis.

DISCUSSION

In this study, we have identified a new endogenous inhibitor of BMP signaling. Previously uncharacterized, *bif1* encodes a C2H2 zinc-finger protein that can translocate to the nucleus. C2H2 ZF represents a family of protein present in all species, from archaea bacteria to humans. Since the discovery of these domains in TFIIIA (Miller et al., 1985), many studies focused their research on this group of proteins, which represent 3% of human proteins (Klug, 2010). This family of proteins is still poorly characterized and no perfect prediction software can determine their molecular function based on their amino acid sequences. It was previously thought that C2H2 domains were only binding DNA until the discovery, in many proteins, of their ability to also bind proteins and RNA (Brayer et al., 2008; Brown, 2005). Moreover, in the same protein, different C2H2 can bind either DNA or proteins, making their studies even more complex. In the case of *bif1*, owing to its capacity to translocate to the nucleus, we hypothesized a predominant role in the nucleus as a transcription factor, but we cannot exclude other functions, such as stabilizing RNA. From this hypothesis, we speculate that *bif1* can inhibit, by binding to DNA, the transcription of specific genes involved in BMP signaling, such as *bmp2b* and *bmp4*.

During gastrulation, BMP ligands and inhibitors are expressed according to opposite gradients, such as *bmp2b* and *bmp7*, and *chordin* and *noggin*. These opposite expressions are responsible for establishing a gradient of BMP activity (Ramel and Hill, 2012). Here, we have identified *bif1* as a new intracellular cell-autonomous inhibitor of BMP signaling that regulates the dorso-ventral patterning during gastrulation. Owing to the expression of BMP members in erythroid

Development (2019) 146, dev164103. doi:10.1242/dev.164103

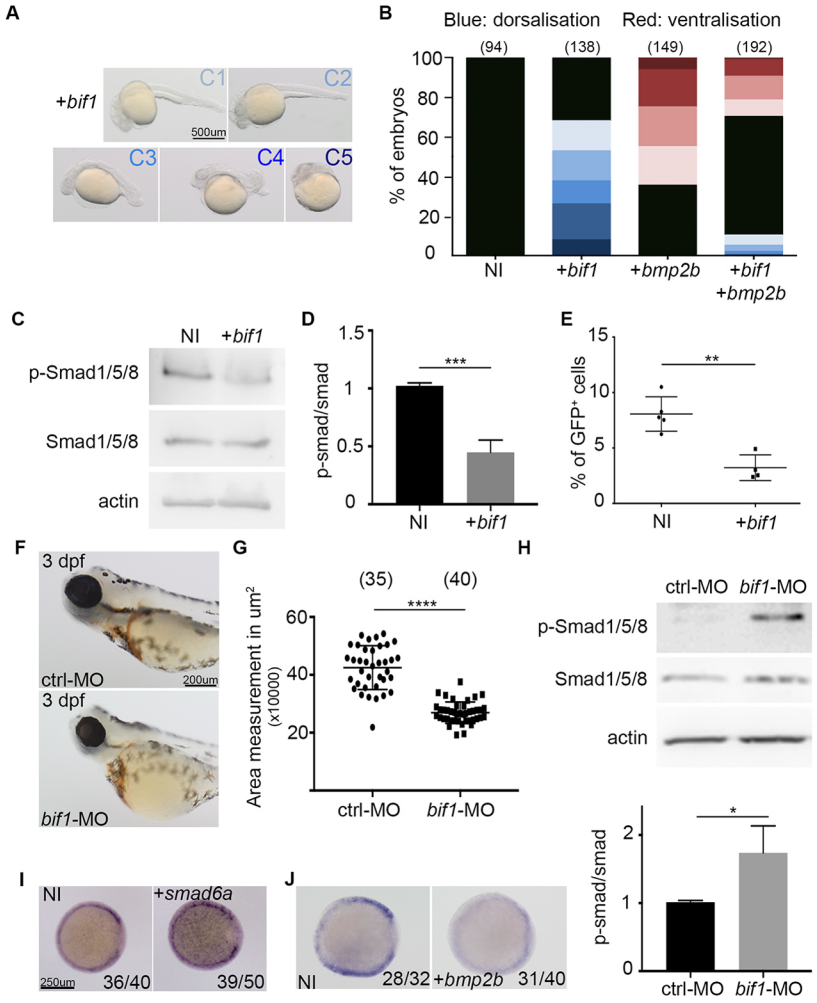

Fig. 5. *bif1* inhibits the BMP signaling pathway. (A) Bright-field images of 24 hpf embryos injected with *bif1* mRNA. The embryos are classified depending of the dorsalization severity. (B) Quantification of embryos exhibiting the corresponding morphologies of dorsalization and ventralization. (C) Western blot of extracted proteins of non-injected embryos or embryos injected with *bif1* mRNA at 6 hpf. (D) Quantitative analysis of western blot data. The values were obtained by dividing the p-Smad protein intensity value by its corresponding Smad intensity value. Data are mean±s.e.m. ***P<0.001. (E) Percentage of eGFP cells obtained by FACS analysis on *Tg(BRE:eGFP)* fishes. Each dot represents a pool of 20 embryos. Data are mean±s.e.m. **P<0.01. (F) Bright-field images from O-dianisidine-stained embryos at 3 dpf. The embryos were injected with control-MO or a *bif1*-MO. (G) Measurement of the left eye size in the embryos in F (the right eyes produce similar results). Each dot represents one single embryo. Data are mean±s.e.m. ****P<0.0001. (H) Western blot of extracted proteins at 23 hpf. The embryos were injected with a control morpholino or a morpholino against *bif1*. The graph below indicates the relative intensity of p-Smad protein levels compared with total Smad proteins. Data are mean±s.e.m. *P<0.05. (I) Whole-mount *in situ* hybridization for *bif1* at 6 hpf in embryos injected with *smad6* mRNA and non-injected controls. (J) Whole-mount *in situ* hybridization for *bif1* at 6 hpf in embryos injected with *bmp2b* mRNA and non-injected controls. Statistical analysis was carried out using an unpaired Student's *t*-test.

progenitors, the role of BMP signaling during erythropoiesis has been deeply investigated. The deletions of *Smad5* or *Bmp4* are embryonic lethal in mice. However, the few mice that survive show strong defects in primitive erythropoiesis (Hegde et al., 2007; Coleman et al., 1969; Winnier et al., 1995), revealing the importance of BMP signaling for the establishment of primitive erythropoiesis. In zebrafish, *smad5* mutants also have defects in primitive erythropoiesis (McReynolds et al., 2007). In these different models, BMP signaling was shown to be required for primitive erythropoiesis. Our experiments show that *bif1* increases the number of *gata1*-positive cells during primitive erythropoiesis, whereas its absence decreases the number of erythrocytes in circulation. This indicates a new role for BMP signaling during primitive erythropoiesis.

Under stress conditions, such as PHZ treatment (induced anemia), the recovery of the mice was delayed in the absence of *Smad5* (Coleman et al., 1969; Lenox et al., 2005; Hegde et al., 2007). Moreover, *Bmp4* is induced in the spleen of mice following anemia (Wu and Paulson, 2010). Through the activation of *Smad5*, *Bmp4* then activates the expansion of erythroid immature BFU-E cells (Perry et al., 2007; Lenox et al., 2005). Moreover, other BMP ligands have been shown to be important during zebrafish stress-induced erythropoiesis, as shown by treatment with ginger, which increases *bmp2b* and *bmp7* expression in the CHT, leading to an increase of erythroid progenitors (Ferri-Lagneau et al., 2012). These data show that, during stress-induced erythropoiesis, BMP signaling is activated in order to increase the expansion of erythroid progenitors. Surprisingly, in our chemically induced anemia experiment, we discovered an expansion of erythroid progenitors in the CHT of embryos injected with *bif1*, where BMP signaling was therefore attenuated. We hypothesize that during stress erythropoiesis, two steps are important for the recovery of erythroid cells. One step needs an increase of BMP signaling to promote erythroid progenitor expansion, whereas a later steps needs to shut down BMP signaling, probably to proceed with normal differentiation. Further studies will be needed to understand this dual role of BMP signaling during erythropoiesis. In mammals, BMP ligands were also shown to be required for the differentiation into erythroid cells from ES cells (Adelman et al., 2002). In fact, BMP4 is needed to activate the transcription of erythroid genes, such as *Eklf* (*Klf1*) and *Gata1*, whereas SMAD6 blocks this induction (Adelman et al., 2002; Schmerer and Evans, 2003). In human cells, BMP2 also increases the number of early BFU-E cells, whereas activin A increases both BFU-E and CFU-E. This result shows that BMP2 is acting in more immature cells (Maguer-Satta et al., 2003). The maturation of zebrafish primitive erythroid cells was delayed or blocked when *bif1* or *smad6a* were overexpressed. Our results are consistent with the previously described role of BMP signaling during erythroid maturation. By blocking BMP signaling, *bif1* blocks erythroid differentiation into mature RBCs, probably by decreasing *gata1*. By contrast, the absence of *bif1* induced a complete absence of primitive erythropoiesis.

We have also found that *bif1* is important for the normal development of HSPCs along the VDA, as *bif1*-morphants exhibit reduced levels of *runx1* and *cmyb* in the hemogenic endothelium.

Development (2019) 146, dev164103. doi:10.1242/dev.164103

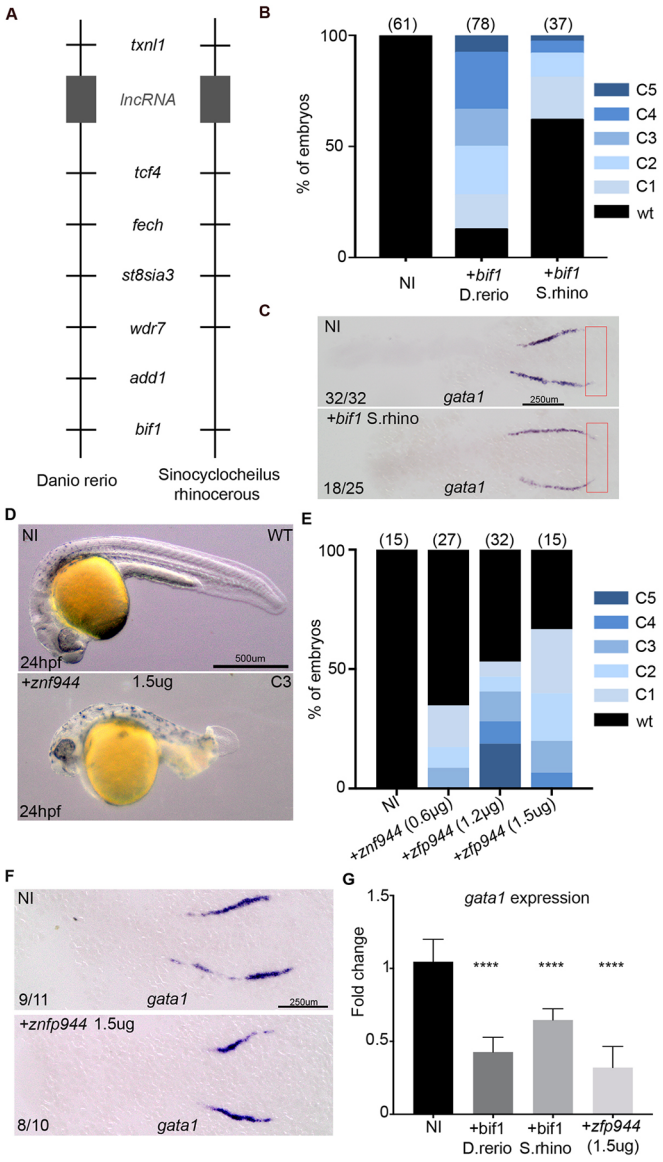

Fig. 6. *bif1* has orthologs in *Sinocyclocheilus rhinocerous* and in *Mus musculus*. (A) Synteny representation of the zebrafish and *Sinocyclocheilus rhinocerous* genome near to *bif1*. (B) Percentage of uninjected embryos and embryos injected with *D. rerio* or *S. rhino bif1* mRNA showing a dorsalization morphology at 24 hpf in zebrafish embryos. (C) Whole-mount *in situ* hybridization for *gata1* at 12 hpf in non-injected embryos or embryos injected with *bif1 S. rhino* mRNA. Red rectangle indicates the region in which *gata1a* is ectopically expressed in *bif1*-overexpressing embryos. (D) Bright-field images of non-injected embryos or embryos injected with *zfp944* mRNA at 24 hpf. (E) Percentage of uninjected and *zfp944*-injected zebrafish embryos showing a dorsalization morphology at 24 hpf. (F) Whole-mount *in situ* hybridization for *gata1* at 12 hpf in non-injected embryos or embryos injected with *zfp944* mRNA. (G) Quantification of *gata1* by qPCR, in 48 hpf embryos, either non-injected or injected with *D. rerio bif1*, *S. rhino bif1* or murine *Zfp944* mRNA (n=3 biological replicates for all). Statistical analysis was carried out using an unpaired Student t-test. Data are mean±s.e.m. ****P<0.0001.

Although BMP signaling positively regulates HSPC emergence (Wilkinson et al., 2009), it was also recently shown that BMP signaling needs to be turned off after HSPC specification for normal HSPC maturation (McGarvey et al., 2017). Therefore, we propose that *bif1* plays such a role during HSPC emergence in the zebrafish embryo.

In summary, we have discovered a new intracellular BMP inhibitor in zebrafish, *bif1*, that is specifically expressed in primitive and definitive hematopoietic lineages during embryogenesis, as well as in adults. We generated a new *bif1:GFP-LT* transgenic reporter that faithfully recapitulates endogenous expression in the embryo only, as we could not observe GFP-LT expression in adult erythroid progenitors.

Through the inhibition of BMP signaling, *bif1* affects dorso-ventral patterning during gastrulation and affects primitive and definitive erythropoiesis, as well as the normal development of HSPCs. This gene is not restricted to *Danio rerio* but is also present in another fish (*S. rhino*), where it probably plays a similar role. Finally, we also found a potential ortholog in the mouse genome, *Zfp944*, that is expressed in the mouse erythroid lineage and induces dorsalization of zebrafish embryos. Further work will be required to understand the precise inhibitory role of this new zinc-finger protein on BMP signaling.

MATERIALS AND METHODS

Zebrafish husbandry

Zebrafish were maintained and bred according to the University of Geneva procedures and authorizations from local veterinary authorities. All experiments were performed using AB* and the following transgenic animals: *Tg(gata1:Dsred)* (Yaqoob et al., 2009), *Tg(BRE:eGFP)* (Collery and Link, 2011) and *cloche*^{m34} mutants (Stainier et al., 1995).

Whole-mount *in situ* hybridization

Whole-mount *in situ* hybridization was performed on 4% paraformaldehyde-fixed embryos. Digoxigenin-labeled and FITC-labeled probes were synthesized using a RNA Labeling kit (SP6/T7; Roche). RNA probes were generated by linearization of TOPO-TA vectors (Invitrogen) containing the PCR-amplified cDNA sequence. Whole-mount *in situ* hybridization was performed as previously described (Thisse et al., 1993). Double whole-mount *in situ* hybridization was performed by using IBT/BCIP (Roche). Embryos were imaged in 100% glycerol using an Olympus MVX10 microscope. The oligonucleotide primers used to clone cDNA for probes are listed in Table S1.

mRNA and morpholino injections

Full-length cDNAs were cloned into the pCS2 vector from which mRNA was synthesized using the mMessage mMachine Kit (Life Technologies). In all experiments, 300 pg of *bif1* mRNA, 100 pg of *bmp2b* or *smad6a* mRNA and 1300 pg of *bif1 S. rhino* were injected into one-cell stage embryos. Except for the rescue experiment with morpholino, *bif1* was injected at 100 pg. Site-directed mutation of *bif1* was performed with the QuickChangeII Site-directed mutagenesis Kit (Agilent Technologies). Morpholino oligonucleotides were purchased from Gene Tools and are listed in Table S2. MO efficiency was tested by reverse transcription polymerase chain reaction (RT-PCR) from total RNA extracted from 10 embryos at 24 hpf using primers listed in Table S1. *bif1-MO* was injected at 17 ng for all experiments except for the rescue experiment, where it was injected at 16 ng.

Western blot

Embryos were lysed in Pierce lysis buffer (Thermo) with a protease and phosphatase inhibitor cocktail (Roche) for 15 min on ice after mechanical disruption. Debris was removed by centrifugation. Samples were then subjected to SDS-polyacrylamide gel electrophoresis and immunoblotting according to standard protocols (Sun et al., 2011), using anti-Smad1/5/9 (1:1000; Creative Diagnostics, DPABH-17143167), anti-phospho-ser463/465-smad1/pser463/465-smad5/pser465/467-smad9 (1:1000; Cell Signaling, 13820) and anti-β-actin (1:25,000; Sigma-Aldrich, A2066) antibodies.

Immunofluorescence

Zebrafish embryos (6 hpf) were fixed in 4% PFA before washes and blocking (PBS+0.1% triton X-100+4% BSA+0.02% NaN_3). The primary anti-HA antibody (1:1000; Abcam, ab18181) was incubated with the samples overnight at 4°C followed by washing and incubation with the

Development (2019) 146, dev164103. doi:10.1242/dev.164103

secondary anti-mouse IgG Alexa-fluor488 antibody (1:1000; Invitrogen, A32723). Nuclei were stained using DAPI (Sigma).

Flow cytometry

Tg(BRE:eGFP) embryos (12 hpf) were dissociated as previously described (Bertrand et al., 2007). Adult WKM were mechanically dissociated. SYTOX Red (Molecular Probes) was used to detect dead cells. Cells were analyzed using a FACSAccuriC6 (BD Biosciences) or a FACS Fortessa (BD Biosciences) and sorted with a FACSAriaII cell sorter (BD Biosciences).

Quantitative real-time PCR and analysis

RNA was extracted using RNeasy minikit (Qiagen) and reverse transcribed into cDNA using a SuperscriptIII kit (Invitrogen). Quantitative real-time PCR (qPCR) was performed using SensiFAST SYBR Lo-ROX kit (Bioline) and run on a QuantStudio3 real-time system (Thermo Fisher). In each sample, levels of expression were normalized to *ef1a*. Statistical analysis was carried out using an unpaired Student's *t*-test in Prism. qPCR experiments were performed in biological triplicates. Primers are listed in Table S1.

Generation of transgenic and mutant animals

For *Tg(bif1:GFP-LT)* fish generation, we cloned a sequence of 1 kb upstream of the start codon in a Tol2 vector containing GFP-LT. For *Tg(Hsp70:bif1-p2a-tfp)* fish generation, we cloned a *bif1*-coding sequence without the stop codon into Tol2 vector containing the HSP70l promoter and a p2a-TFP fusion cassette (a kind gift from Benjamin Martin, Stony Brooks University, NY, USA). Zebrafish embryos were injected with 40 pg of the final Tol2 vector, along with 40 pg Tol2 transposase mRNA. Injected F0 adults were mated to AB* or *Tg(gata1:Dsred)*, and the F1 offspring were screened to assess germline integration of the Tol2 construct. Primers are listed in Table S1.

Phenylhydrazine treatment and O-dianisidine staining

Phenylhydrazine (0.5 µg/ml final) was added into the incubation medium of 33 hpf zebrafish embryos, followed by extensive washes at 48 hpf. Detection of hemoglobin by o-dianisidine was performed as described previously (Ransom et al., 1996).

May–Grünwald–Giemsa staining of primitive RBCs

After tail clipping using a scalpel, blood cells were collected by pipetting, in 0.9× PBS and 1% BSA (Sigma-Aldrich). Then they were cytospun onto slides by centrifugation at 23 ***g*** for 5 min using a shandon cytospin 2. The slides were then air-dried and subjected to May–Grünwald–Giemsa staining according to a standard protocol (Bertrand et al., 2007).

Acknowledgements

We thank Dr Claire Pouget for the *acta2* probe, Dr Richard Fish for the *ntla* and *bmp4* probes, and Dr Benjamin Martin for the *evx1* probe and the tol2-hsp70l-p2A-TFP vector. We also acknowledge C. Pasche and C. Compebine for excellent technical support. We thank M. Cavanaugh and Dr Stefania Nicoli for allowing us to use their lab facilities.

Competing interests

The authors declare no competing or financial interests.

Author contributions

Conceptualization: J.Y.B.; Methodology: J.J.G.; Validation: J.J.G.; Formal analysis: J.J.G., C.B.M., J.Y.B.; Investigation: J.J.G., C.B.M.; Writing - original draft: J.J.G., J.Y.B.; Visualization: J.J.G., C.B.M.; Supervision: J.Y.B.; Project administration: J.Y.B.; Funding acquisition: J.Y.B.

Funding

This project was primarily funded by Carigest. J.Y.B. was endorsed by a Chair in Life Sciences funded by the Gabriella Giorgi-Cavaglieri Foundation and is also funded by the Schweizerischer Nationalfonds zur Förderung der Wissenschaftlichen Forschung (31003_166515).

Supplementary information

Supplementary information available online at
http://dev.biologists.org/lookup/doi/10.1242/dev.164103.supplemental

References

Adelman, C. A., Chattopadhyay, S. and Bieker, J. J. (2002). The BMP/BMPR/Smad pathway directs expression of the erythroid-specific EKLF and GATA1 transcription factors during embryoid body differentiation in serum-free media. *Development* **129**, 539-549.

Al-Adhami Ma, K. Y. (1977). Ontogenesis of haematopoietic sites in *Brachydanio rerio*. *Dev. Growth Diff.* **19**, 171-179.

Bertrand, J. Y., Kim, A. D., Violette, E. P., Stachura, D. L., Cisson, J. L. and Traver, D. (2007). Definitive hematopoiesis initiates through a committed erythromyeloid progenitor in the zebrafish embryo. *Development* **134**, 4147-4156.

Bertrand, J. Y., Chi, N. C., Santoso, B., Teng, S., Stainier, D. Y. R. and Traver, D. (2010). Haematopoietic stem cells derive directly from aortic endothelium during development. *Nature* **464**, 108-111.

Blank, U., Karlsson, G., Moody, J. L., Utsugisawa, T., Magnusson, M., Singbrant, S., Larsson, J. and Karlsson, S. (2006). Smad7 promotes self-renewal of hematopoietic stem cells. *Blood* **108**, 4246-4254.

Brayer, K. J. and Segal, D. J. (2008). Keep your fingers off my DNA: protein-protein interactions mediated by C2H2 zinc finger domains. *Cell Biochem. Biophys.* **50**, 111-131.

Brayer, K. J., Kulshreshtha, S. and Segal, D. J. (2008). The protein-binding potential of C2H2 zinc finger domains. *Cell Biochem. Biophys.* **51**, 9-19.

Brown, R. S. (2005). Zinc finger proteins: getting a grip on RNA. *Curr. Opin. Struct. Biol.* **15**, 94-98.

Cannon, J. E., Place, E. S., Eve, A. M. J., Bradshaw, C. R., Sesay, A., Morrell, N. W. and Smith, J. C. (2013). Global analysis of the haematopoietic and endothelial transcriptome during zebrafish development. *Mech. Dev.* **130**, 122-131.

Chadwick, K., Shojaei, F., Gallacher, L. and Bhatia, M. (2005). Smad7 alters cell fate decisions of human hematopoietic repopulating cells. *Blood* **105**, 1905-1915.

Chen, D., Zhao, M., Harris, S. E. and Mi, Z. (2004). Signal transduction and biological functions of bone morphogenetic proteins. *Front. Biosci.* **9**, 349-358.

Coleman, D. L., Russell, E. S. and Levin, E. Y. (1969). Enzymatic studies of the hemopoietic defect in flexed mice. *Genetics* **61**, 631-642.

Collery, R. F. and Link, B. A. (2011). Dynamic smad-mediated BMP signaling revealed through transgenic zebrafish. *Dev. Dyn.* **240**, 712-722.

Detrich, H. W., III, Kieran, M. W., Chan, F. Y., Barone, L. M., Yee, K., Rundstadler, J. A., Pratt, S., Ransom, D. and Zon, L. I. (1995). Intraembryonic hematopoietic cell migration during vertebrate development. *Proc. Natl Acad. Sci. USA* **92**, 10713-10717.

Ferri-Lagneau, K. F., Moshal, K. S., Grimes, M., Zahora, B., Lv, L., Sang, S. and Leung, T. C. (2012). Ginger stimulates hematopoiesis via Bmp pathway in zebrafish. *PLoS ONE* **7**, e39327.

Fürthauer, M., Thisse, B. and Thisse, C. (1999). Three different noggin genes antagonize the activity of bone morphogenetic proteins in the zebrafish embryo. *Dev. Biol.* **214**, 181-196.

Gupta, S., Zhu, H., Zon, L. I. and Evans, T. (2006). BMP signaling restricts hemato-vascular development from lateral mesoderm during somitogenesis. *Development* **133**, 2177-2187.

Hammerschmidt, M., Pelegri, F., Mullins, M. C., Kane, D. A., Van Eeden, F. J., Granato, M., Brand, M., Furutani-Seiki, M., Haffter, P., Heisenberg, C. P. et al. (1996). dino and mercedes, two genes regulating dorsal development in the zebrafish embryo. *Development* **123**, 95-102.

Hegde, S., Lenox, L. E., Lariviere, A., Porayette, P., Perry, J. M., Yon, M. and Paulson, R. F. (2007). An intronic sequence mutated in flexed-tail mice regulates splicing of Smad5. *Mamm. Genome* **18**, 852-860.

Hild, M., Dick, A., Rauch, G. J., Meier, A., Bouwmeester, T., Haffter, P. and Hammerschmidt, M. (1999). The smad5 mutation somitabun blocks Bmp2b signaling during early dorsoventral patterning of the zebrafish embryo. *Development* **126**, 2149-2159.

Kang, Y.-J., Shin, J.-W., Yoon, J.-H., Oh, I.-H., Lee, S.-P., Kim, S.-Y., Park, S. H. and Mamura, M. (2012). Inhibition of erythropoiesis by Smad6 in human cord blood hematopoietic stem cells. *Biochem. Biophys. Res. Commun.* **423**, 750-756.

Katagiri, T., Imada, M., Yanai, T., Suda, T., Takahashi, N. and Kamijo, R. (2002). Identification of a BMP-responsive element in Id1, the gene for inhibition of myogenesis. *Genes Cells* **7**, 949-960.

Keller, G., Lacaud, G. and Robertson, S. (1999). Development of the hematopoietic system in the mouse. *Exp. Hematol.* **27**, 777-787.

Kishimoto, Y., Lee, K. H., Zon, L., Hammerschmidt, M. and Schulte-Merker, S. (1997). The molecular nature of zebrafish swirl: BMP2 function is essential during early dorsoventral patterning. *Development* **124**, 4457-4466.

Kissa, K. and Herbomel, P. (2010). Blood stem cells emerge from aortic endothelium by a novel type of cell transition. *Nature* **464**, 112-115.

Klug, A. (2010). The discovery of zinc fingers and their development for practical applications in gene regulation and genome manipulation. *Q. Rev. Biophys.* **43**, 1-21.

Kondo, M. (2007). Bone morphogenetic proteins in the early development of zebrafish. *FEBS J.* **274**, 2960-2967.

Lenox, L. E., Perry, J. M. and Paulson, R. F. (2005). BMP4 and Madh5 regulate the erythroid response to acute anemia. *Blood* **105**, 2741-2748.

Liao, E. C., Paw, B. H., Oates, A. C., Pratt, S. J., Postlethwait, J. H. and Zon, L. I. (1998). SCL/Tal-1 transcription factor acts downstream of cloche to specify hematopoietic and vascular progenitors in zebrafish. *Genes Dev.* **12**, 621-626.

Liu, B., Sun, Y., Jiang, F., Zhang, S., Wu, Y., Lan, Y., Yang, X. and Mao, N. (2003). Disruption of Smad5 gene leads to enhanced proliferation of high-proliferative potential precursors during embryonic hematopoiesis. *Blood* **101**, 124-133.
Long, Q., Meng, A., Wang, H., Jessen, J. R., Farrell, M. J. and Lin, S. (1997). GATA-1 expression pattern can be recapitulated in living transgenic zebrafish using GFP reporter gene. *Development* **124**, 4105-4111.
Maguer-Satta, V., Bartholin, L., Jeanpierre, S., Ffrench, M., Martel, S., Magaud, J.-P. and Rimokh, R. (2003). Regulation of human erythropoiesis by activin A, BMP2, and BMP4, members of the TGFbeta family. *Exp. Cell Res.* **282**, 110-120.
Mcgarvey, A. C., Rybtsov, S., Souilhol, C., Tamagno, S., Rice, R., Hills, D., Godwin, D., Rice, D., Tomlinson, S. R. and Medvinsky, A. (2017). A molecular roadmap of the AGM region reveals BMPER as a novel regulator of HSC maturation. *J. Exp. Med.* **214**, 3731-3751.
Mcgrath, K. E., Frame, J. M., Fromm, G. J., Koniski, A. D., Kingsley, P. D., Little, J., Bulger, M. and Palis, J. (2011). A transient definitive erythroid lineage with unique regulation of the beta-globin locus in the mammalian embryo. *Blood* **117**, 4600-4608.
Mcreynolds, L. J., Gupta, S., Figueroa, M. E., Mullins, M. C. and Evans, T. (2007). Smad1 and Smad5 differentially regulate embryonic hematopoiesis. *Blood* **110**, 3881-3890.
Medvinsky, A. and Dzierzak, E. (1996). Definitive hematopoiesis is autonomously initiated by the AGM region. *Cell* **86**, 897-906.
Miller, J., Mclachlan, A. D. and Klug, A. (1985). Repetitive zinc-binding domains in the protein transcription factor IIIA from Xenopus oocytes. *EMBO J.* **4**, 1609-1614.
Mullins, M. C., Hammerschmidt, M., Kane, D. A., Odenthal, J., Brand, M., Van Eeden, F. J., Furutani-Seiki, M., Granato, M., Haffter, P., Heisenberg, C. P. et al. (1996). Genes establishing dorsoventral pattern formation in the zebrafish embryo: the ventral specifying genes. *Development* **123**, 81-93.
Murayama, E., Kissa, K., Zapata, A., Mordelet, E., Briolat, V., Lin, H.-F., Handin, R. I. and Herbomel, P. (2006). Tracing hematopoietic precursor migration to successive hematopoietic organs during zebrafish development. *Immunity* **25**, 963-975.
Nandakumar, S. K., Ulirsch, J. C. and Sankaran, V. G. (2016). Advances in understanding erythropoiesis: evolving perspectives. *Br. J. Haematol.* **173**, 206-218.
Palis, J. (2014). Primitive and definitive erythropoiesis in mammals. *Front. Physiol.* **5**, 3.
Palis, J., Robertson, S., Kennedy, M., Wall, C. and Keller, G. (1999). Development of erythroid and myeloid progenitors in the yolk sac and embryo proper of the mouse. *Development* **126**, 5073-5084.
Perry, J. M., Harandi, O. F. and Paulson, R. F. (2007). BMP4, SCF, and hypoxia cooperatively regulate the expansion of murine stress erythroid progenitors. *Blood* **109**, 4494-4502.
Pomreinke, A. P., Soh, G. H., Rogers, K. W., Bergmann, J. K., Blassle, A. J. and Müller, P. (2017). Dynamics of BMP signaling and distribution during zebrafish dorsal-ventral patterning. *eLife* **6**, e25861.
Pyati, U. J., Cooper, M. S., Davidson, A. J., Nechiporuk, A. and Kimelman, D. (2006). Sustained Bmp signaling is essential for cloaca development in zebrafish. *Development* **133**, 2275-2284.
Ramel, M.-C. and Hill, C. S. (2012). Spatial regulation of BMP activity. *FEBS Lett.* **586**, 1929-1941.
Ransom, D. G., Haffter, P., Odenthal, J., Brownlie, A., Vogelsang, E., Kelsh, R. N., Brand, M., Van Eeden, F. J., Furutani-Seiki, M., Granato, M. et al. (1996). Characterization of zebrafish mutants with defects in embryonic hematopoiesis. *Development* **123**, 311-319.
Sankaran, V. G. and Orkin, S. H. (2013). The switch from fetal to adult hemoglobin. *Cold Spring Harb Perspect Med* **3**, a011643.
Sasai, Y., Lu, B., Steinbeisser, H., Geissert, D., Gont, L. K. and De Robertis, E. M. (1994). Xenopus chordin: a novel dorsalizing factor activated by organizer-specific homeobox genes. *Cell* **79**, 779-790.
Schmerer, M. and Evans, T. (2003). Primitive erythropoiesis is regulated by Smad-dependent signaling in postgastrulation mesoderm. *Blood* **102**, 3196-3205.
Schmid, B., Furthauer, M., Connors, S. A., Trout, J., Thisse, B., Thisse, C. and Mullins, M. C. (2000). Equivalent genetic roles for bmp7/snailhouse and bmp2b/swirl in dorsoventral pattern formation. *Development* **127**, 957-967.
Shafizadeh, E., Peterson, R. T. and Lin, S. (2004). Induction of reversible hemolytic anemia in living zebrafish using a novel small molecule. *Comp. Biochem. Physiol. C Toxicol. Pharmacol.* **138**, 245-249.
Smith, W. C. and Harland, R. M. (1992). Expression cloning of noggin, a new dorsalizing factor localized to the Spemann organizer in Xenopus embryos. *Cell* **70**, 829-840.
Song, Y., Wang, M., Mao, F., Shao, M., Zhao, B., Song, Z., Shao, C. and Gong, Y. (2013). Knockdown of Pnpla6 protein results in motor neuron defects in zebrafish. *Dis. Model. Mech.* **6**, 404-413.
Stainier, D. Y., Weinstein, B. M., Detrich, H. W., III, Zon, L. I. and Fishman, M. C. (1995). Cloche, an early acting zebrafish gene, is required by both the endothelial and hematopoietic lineages. *Development* **121**, 3141-3150.
Stickney, H. L., Imai, Y., Draper, B., Moens, C. and Talbot, W. S. (2007). Zebrafish bmp4 functions during late gastrulation to specify ventroposterior cell fates. *Dev. Biol.* **310**, 71-84.
Sun, Y., Wloga, D. and Dougan, S. T. (2011). Embryological manipulations in zebrafish. *Methods Mol. Biol.* **770**, 139-184.
Tadros, W. and Lipshitz, H. D. (2009). The maternal-to-zygotic transition: a play in two acts. *Development* **136**, 3033-3042.
Thisse, C., Thisse, B., Schilling, T. F. and Postlethwait, J. H. (1993). Structure of the zebrafish snail1 gene and its expression in wild-type, spadetail and no tail mutant embryos. *Development* **119**, 1203-1215.
Thompson, M. A., Ransom, D. G., Pratt, S. J., Maclennan, H., Kieran, M. W., Detrich, H. W., III, Vail, B., Huber, T. L., Paw, B., Brownlie, A. J. et al. (1998). The cloche and spadetail genes differentially affect hematopoiesis and vasculogenesis. *Dev. Biol.* **197**, 248-269.
Wilkinson, R. N., Pouget, C., Gering, M., Russell, A. J., Davies, S. G., Kimelman, D. and Patient, R. (2009). Hedgehog and Bmp polarize hematopoietic stem cell emergence in the zebrafish dorsal aorta. *Dev. Cell* **16**, 909-916.
Willett, C. E., Cortes, A., Zuasti, A. and Zapata, A. G. (1999). Early hematopoiesis and developing lymphoid organs in the zebrafish. *Dev. Dyn.* **214**, 323-336.
Winnier, G., Blessing, M., Labosky, P. A. and Hogan, B. L. (1995). Bone morphogenetic protein-4 is required for mesoderm formation and patterning in the mouse. *Genes Dev.* **9**, 2105-2116.
Wolfe, S. A., Nekludova, L. and Pabo, C. O. (2000). DNA recognition by Cys2His2 zinc finger proteins. *Annu. Rev. Biophys. Biomol. Struct.* **29**, 183-212.
Wu, D. C. and Paulson, R. F. (2010). Hypoxia regulates BMP4 expression in the murine spleen during the recovery from acute anemia. *PLoS One* **5**, e11303.
Wu, M., Chen, G. and Li, Y.-P. (2016). TGF-beta and BMP signaling in osteoblast, skeletal development, and bone formation, homeostasis and disease. *Bone Res.* **4**, 16009.
Yang, Y. and Thorpe, C. (2011). BMP and non-canonical Wnt signaling are required for inhibition of secondary tail formation in zebrafish. *Development* **138**, 2601-2611.
Yaqoob, N., Holotta, M., Prem, C., Kopp, R. and Schwerte, T. (2009). Ontogenetic development of erythropoiesis can be studied non-invasively in GATA-1:DsRed transgenic zebrafish. *Comp. Biochem. Physiol. A Mol. Integr. Physiol.* **154**, 270-278.
Zhang, L., Ye, Y., Long, X., Xiao, P., Ren, X. and Yu, J. (2016). BMP signaling and its paradoxical effects in tumorigenesis and dissemination. *Oncotarget* **7**, 78206-78218.

Supplemental Figures

Figure S1

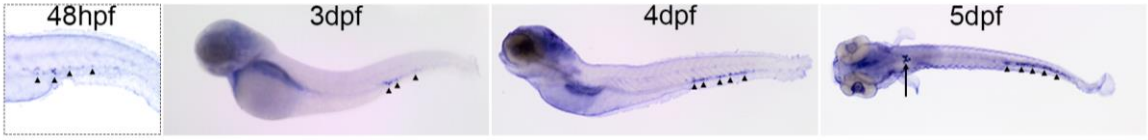

Figure S1. *bif1* is expressed in erythropoietic tissue. Lateral picture of WISH against *bif1* at 3dpf, 4dpf and at 5dpf on a dorsal view. Black arrowheads represent the expression of *bif1* in the CHT. Black arrow shows the expression of *bif1* in the glomerulus.

Figure S2

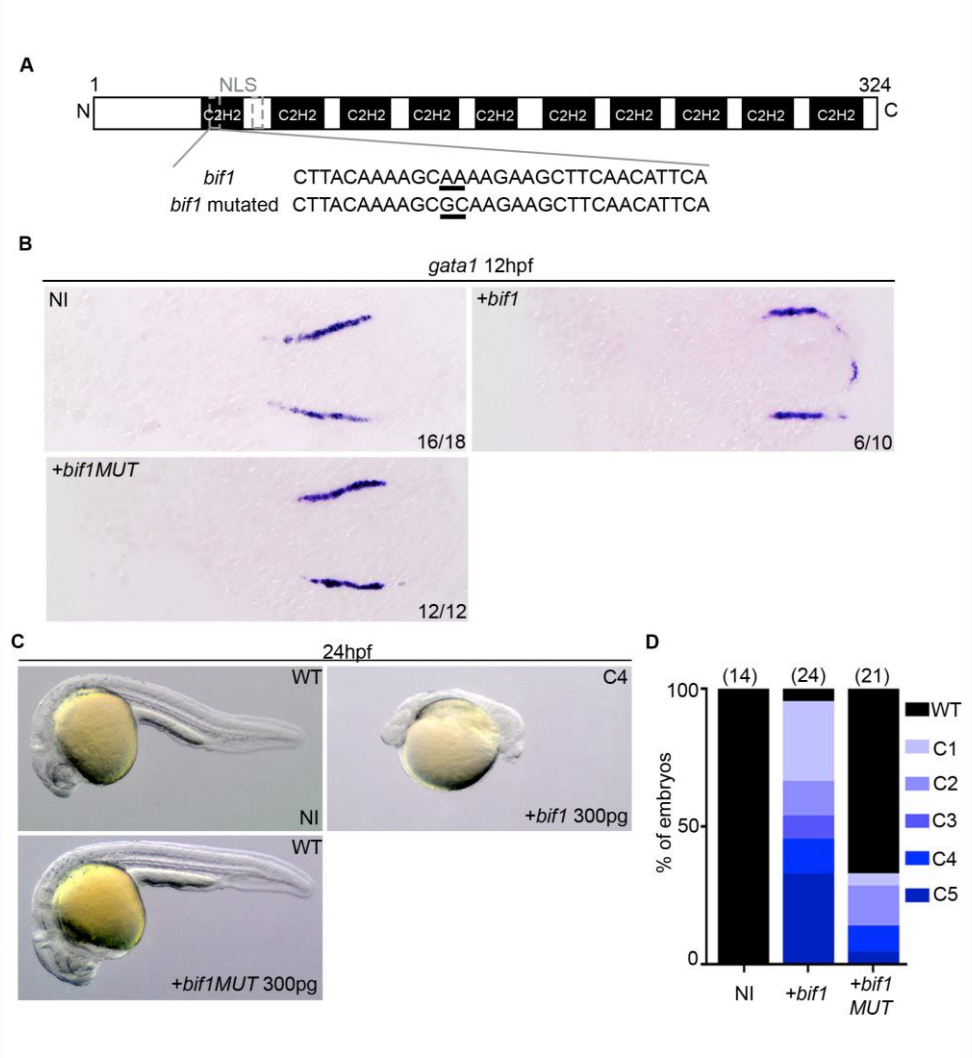

Figure S2. A mutation in bif1-NLS affects its function. (A) Representation of bif1 protein and its nucleotide sequence in the NLS region. The mutation that substitutes a lysine (AAA) to an alanine (GCA) is underlined. (B) WISH against *gata1* at 12hpf embryos injected or not with *bif1* or *bif1* mutated. (C) Bright field images of 24hpf embryos injected or not with *bif1* or *bif1* mutated. (D) Quantification of embryos exhibiting dorsalized morphologies.

Figure S3

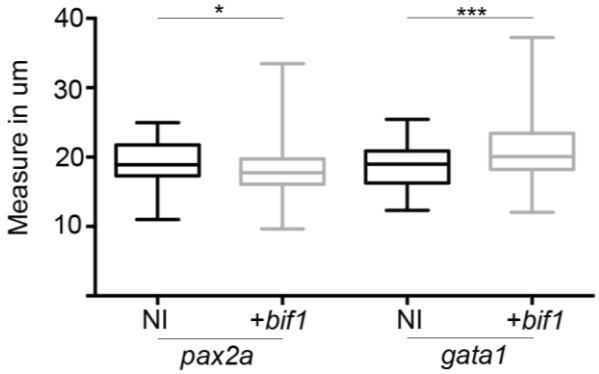

Figure S3. *bif1* regulates the balance between erythroid and pronephric lineages. The graph represents *gata1* and *pax2a* width measurement. Statistical analysis was completed using an un-paired Student t test. Data represents mean ± SEM *P < 0.05, ± SEM ***P < 0.001.

Figure S4

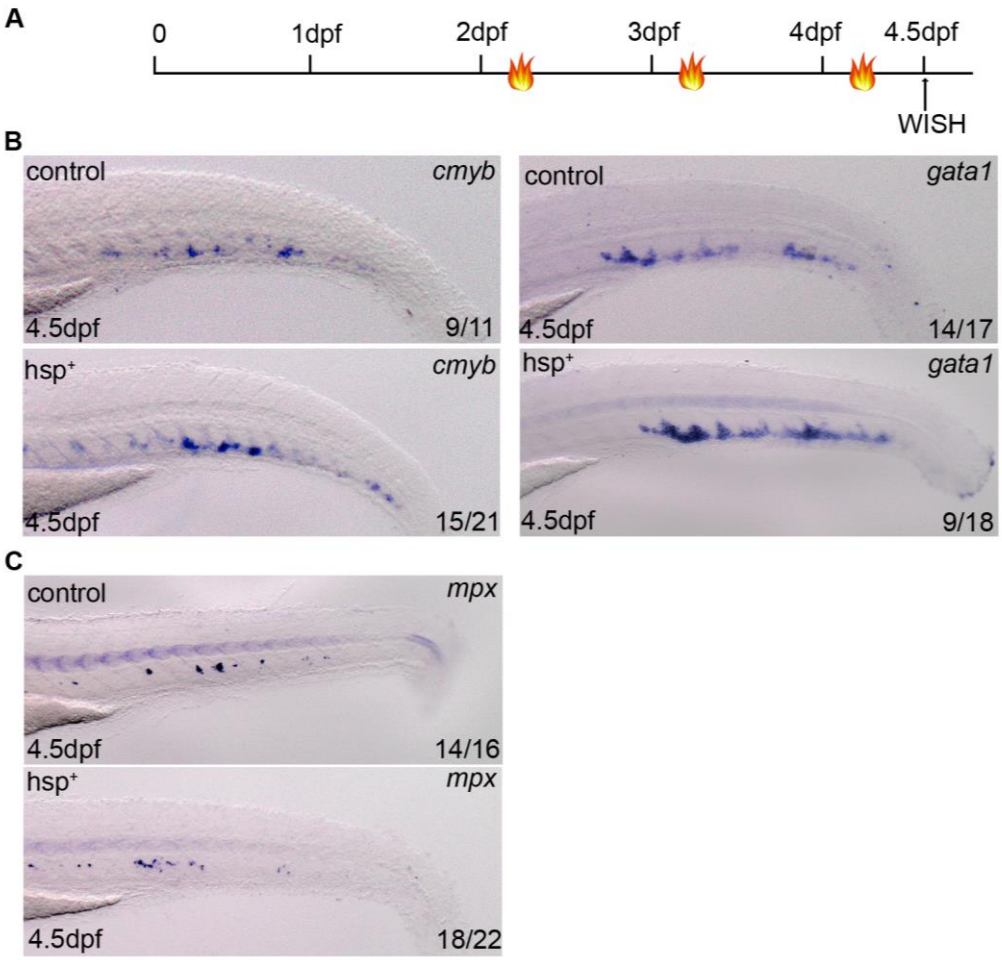

Figure S4. Definitive hematopoiesis is slightly affected by *bif1* overexpression. A. Experimental outline of the overexpression of bif1 by heat shock at 38°C during 45 minutes (flames). B. WISH against *cmyb* and *gata1* at 4.5dpf in control or Tg(Hsp70:*bif1*-p2a-*tfp*) embryos. C. WISH against *mpx* at 4.5dpf in control or Tg(Hsp70:*bif1*-p2a-*tfp*) embryos.

Figure S5

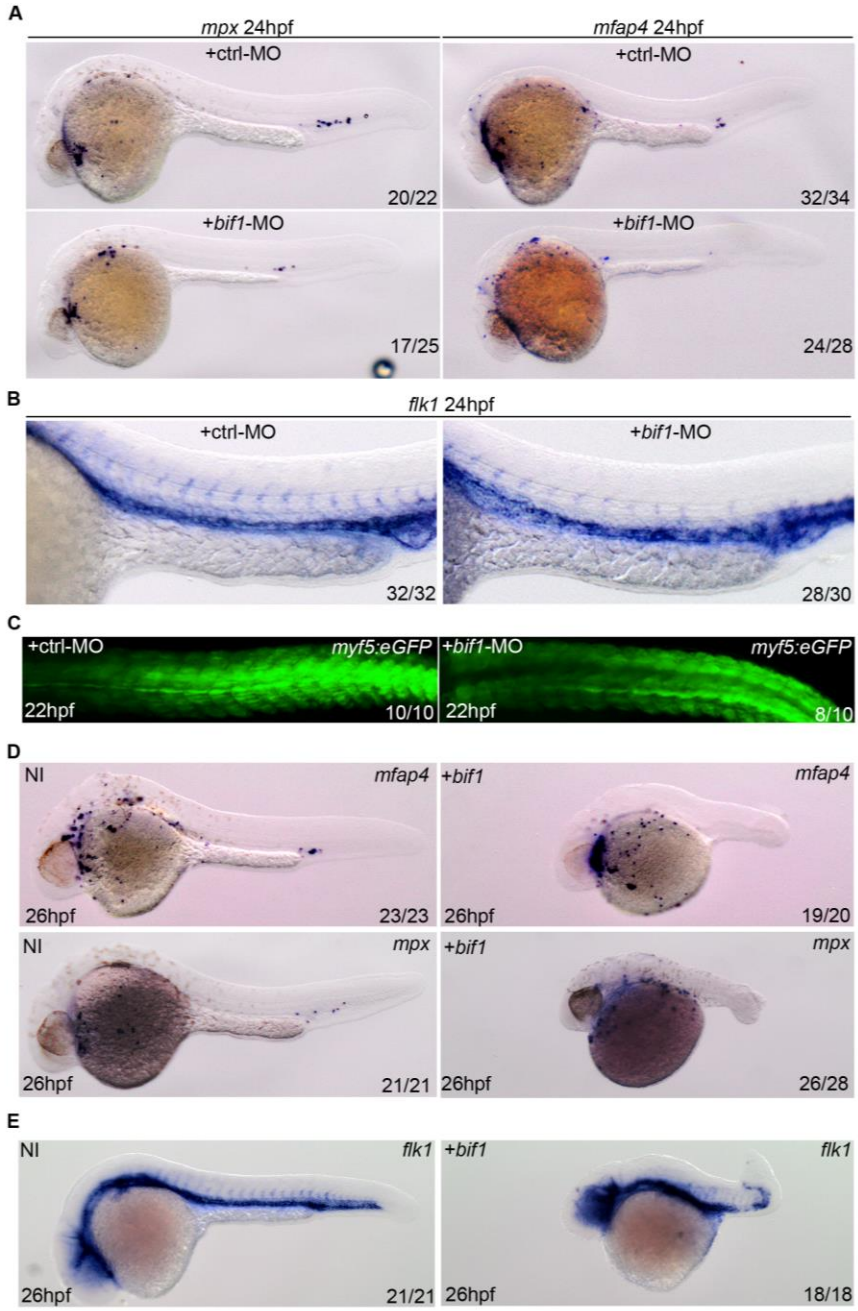

Figure S5. Primitive myelopoiesis and vasculogenesis are not affected in *bif1*-morphants. A. WISH against *mpx* and *mfap4* at 24hpf in embryos injected with ctrl-MO or *bif1*-MO. B. WISH against *flk1* in embryos injected with ctrl-MO or *bif1*-MO. C. Pictures of the tail region of Tg(*myf5*:*eGFP*) embryos, at 22hpf, injected with ctrl-MO or *bif1*-MO. D. WISH against *mpx* and *mfap4* at 24hpf in embryos injected with *bif1* mRNA. E. WISH against *flk1* in embryos injected or not with *bif1* mRNA.

Figure S6

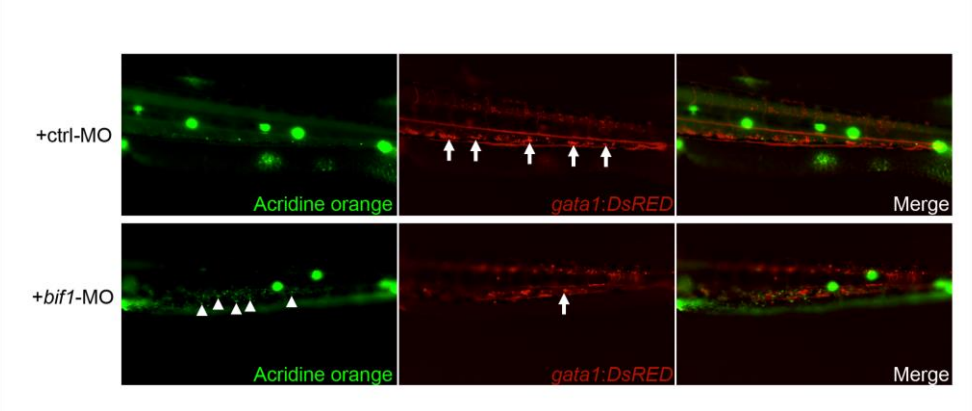

Figure S6. *bif1* is important for cell-survival in the CHT. Acridine orange assay at 4dpf embryos (Zoom on the CHT region). These embryos were injected with a control morpholino or a morpholino against *bif1*. White arrows show gata1-positive cells present in the CHT. White arrowheads represent acridine orange-positive cells.

Figure S7

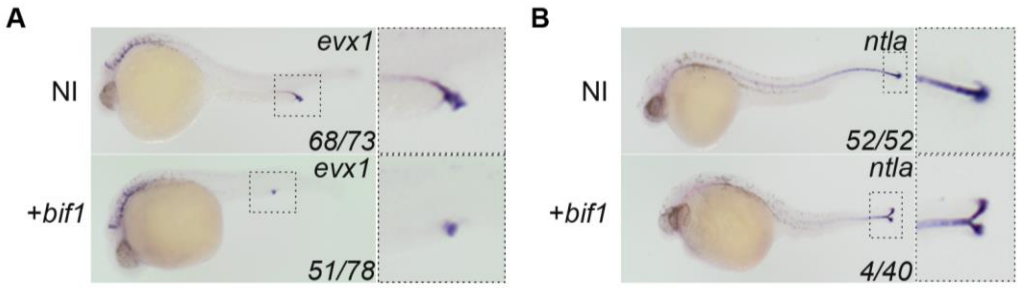

Figure S7. *bif1* alters cloaca development and initiates the formation of an ectopic tail. (A) WISH of *evx1*, expressed in the cloaca and (B) *ntla*, expressed in the notochord, at 23hpf. Enlarged images on the right represent the region indicated by dashed outline box.

Figure S8

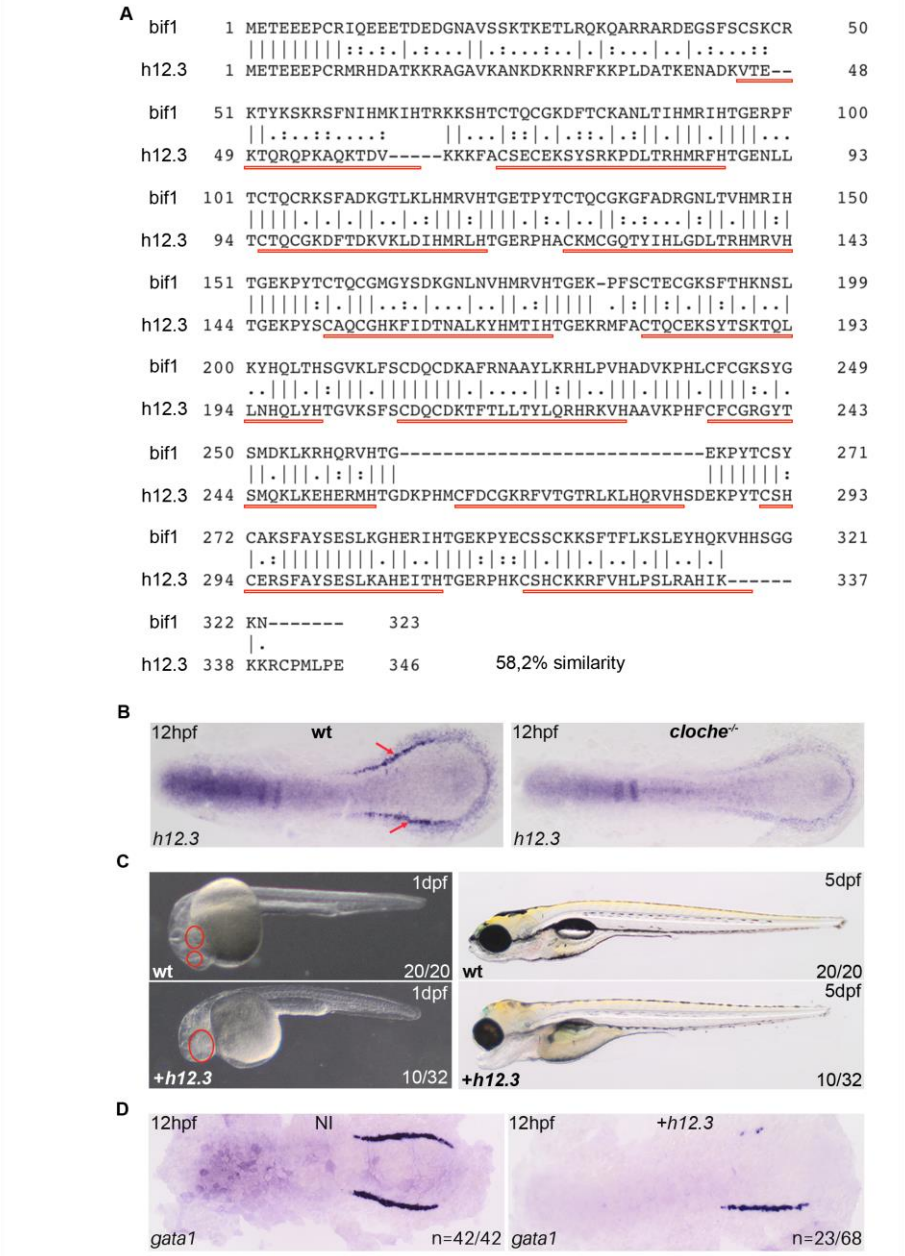

Figure S8. *si:ch73-299h12.3*, a paralogue of *bif1*, induces cyclopia but not dorsalization. A. Protein alignment between bif1 and si:ch73-299h12.3 (h12.3). The protein similarity is 58,2%. The red lines represent the C2H2 domains of bif1. B. *h12.3* is, similar to *bif1*, expressed and in the posterior LPM and its expression is lost in *cloche* mutant. C. Bright field pictures of embryos, at 1dpf and 5dpf, injected or not with *h12.3* mRNA. Red circles mark the eyes; in *h12.3*-injected embryos, only one cyclopic eye is formed. D. WISH against *gata1* at 12hpf in embryos injected with *h12.3*.

Figure S9

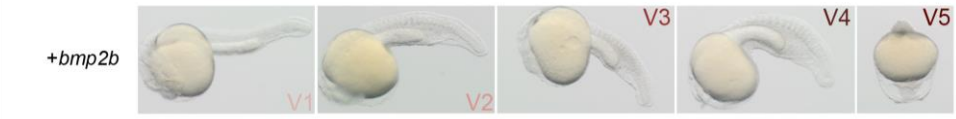

Figure S9. Ventralization effect of *bmp2b*. Ventralized morphology in 24hpf embryos injected with *bmp2b* mRNA. The embryos have been classified following five categories by order of severity (V1 to V5).

Figure S10

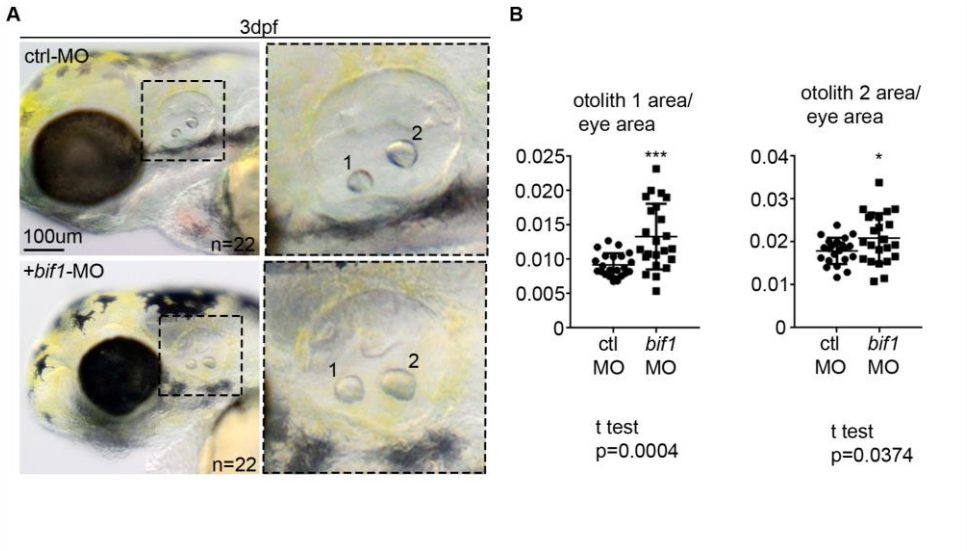

Figure S10. The eye phenotype in *bif1*-morphants is not due to a developmental delay. A. Bright field pictures of the head region of embryos injected with the control morpholino or *bif1*-MO. Enlarged images on the right represent the region indicated by dashed outline box. B. Quantification of otholiths area related to eyes area. Statistical analysis was completed using an un-paired Student t test. Data represents mean ± SEM *P < 0.05, ± SEM ***P < 0.001.

Figure S11

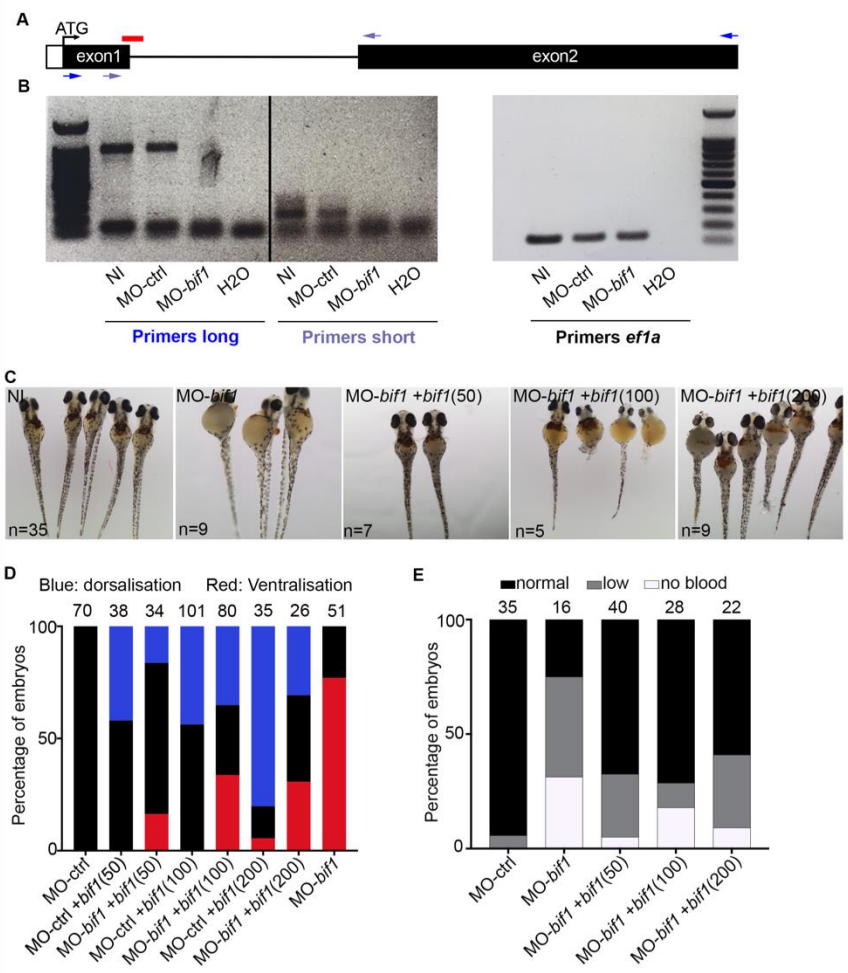

Figure S11. *bif1* knockdown is rescued by co-injection with *bif1* mRNA. A. Schematic representation of the genomic structure of *bif1*. The red line corresponds to the morpholino-targeted site. Dark and light blue arrows correspond to the primers amplifying a long (972 nucleotides) and a short product (224 nucleotides), respectively. The size of the intron is 1122 nucleotides. B. PCR on cDNA obtained from embryos at 24hpf, injected with MO-control or MO-*bif1*, or non-injected. In *bif1*-morphants, the wild-type band disappears, suggesting retention of the intron. C. Bright-field pictures of embryos at 3dpf stained with O-dianisidine. D. Quantification of embryos exhibiting the corresponding morphologies, dorsalization and ventralization (smaller eyes) at 3dpf. The numbers of embryos are indicated in parentheses. E. Quantification of embryos after O-dianisidine staining at 3dpf.

Figure S12

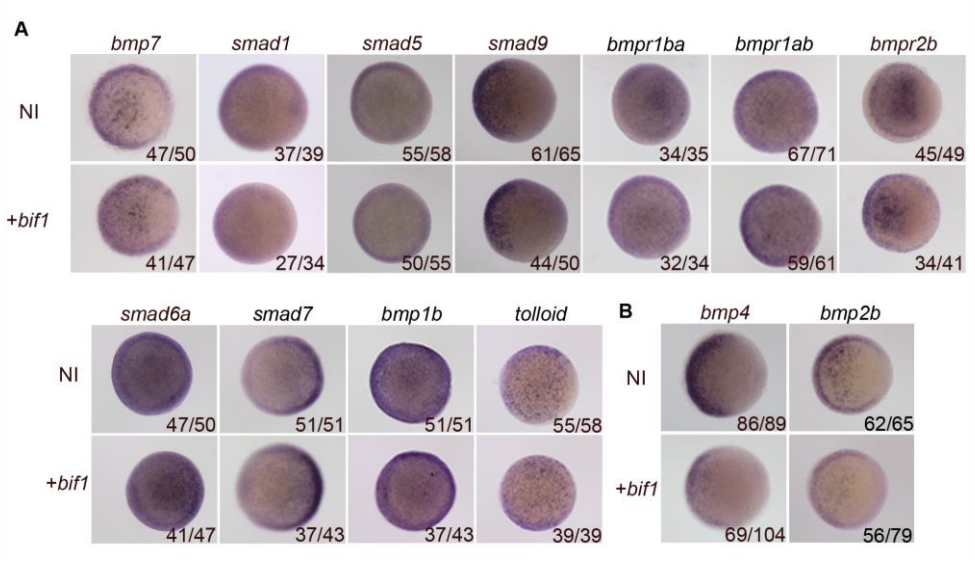

Figure S12. *bif1* alters *bmp2b* and *bmp4* expression. A. WISH on 6hpf embryos injected with *bif1* mRNA compared to control non-injected embryos (wild-type). We tested the following probes: *bmp7*, *smad1*, *smad5*, *smad9*, *bmpr1ba*, *bmpr1ab*, *bmpr2b*, *smad6*, *smad7*, *bmp1b*, *tolloid.* B. WISH on 6hpf embryos against *bmp4* and *bmp2b* injected with bif1 compared to control embryos (wild-type).

Figure S13

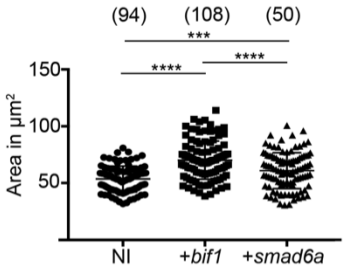

Figure S13. *Smad6a* alters/controls erythroid maturation similarly to *bif1*. Area of circulating red blood cells from May-Grünwald Giemsa staining, after cytospin, of 4dpf wild-type embryos and embryos injected with *bif1* or *smad6a* mRNA. Statistical analysis was completed using an un-paired Student t test. Data represents mean ± SEM ***P < 0.001, ± SEM ****P < 0.0001

Figure S14

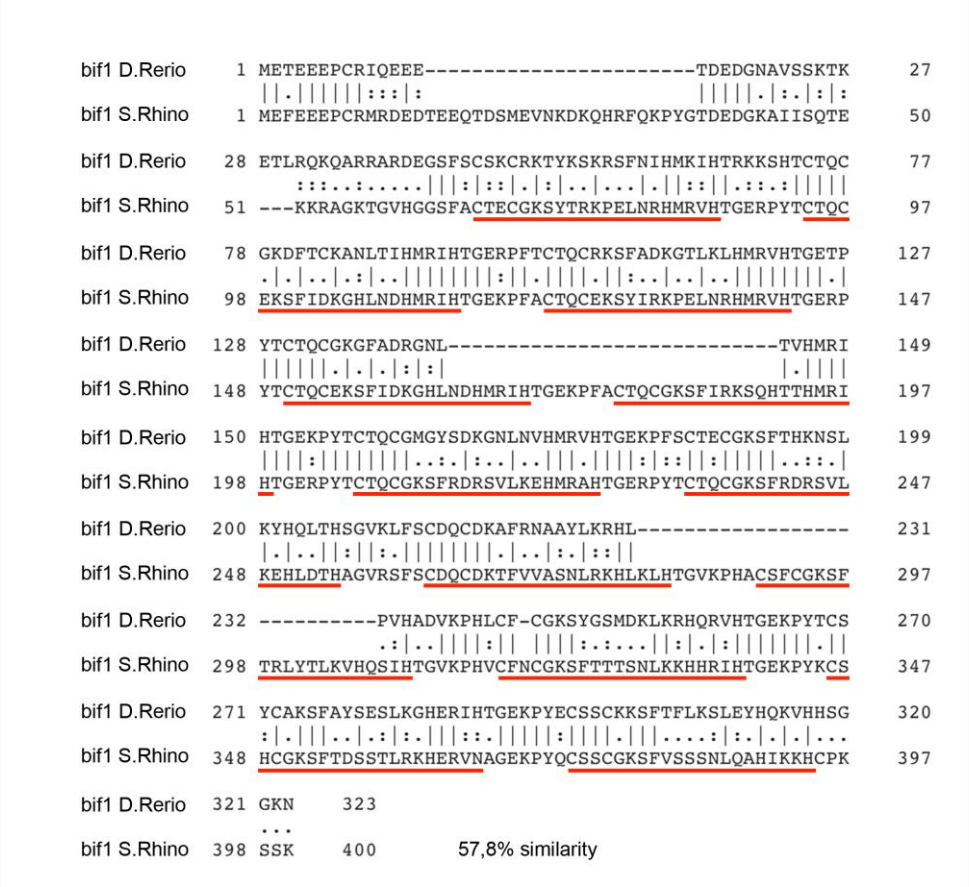

Figure S14. Protein alignment between *bif1* and *si:ch73-299h12.3 (h12.3)*. The protein similarity is 57,8%. The red lines represent the C2H2 domain of *bif1*.

Figure S15

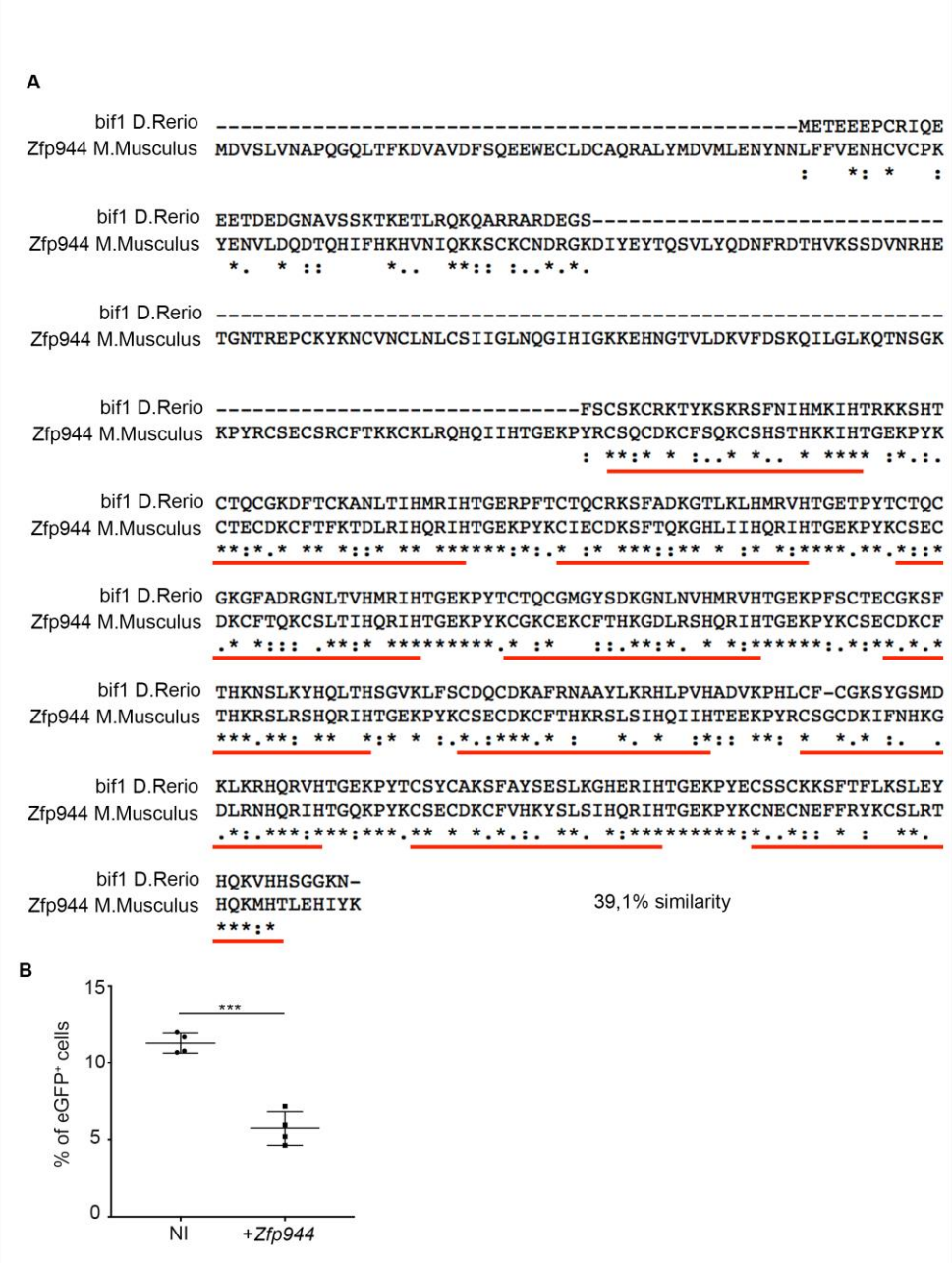

Figure S15. *Zfp944* is a potential orthologue of *bif1* in *M.musculus*. A. Protein alignment between *bif1* and *Zfp944* (http://www.genome.jp/tools-bin/clustalw). The red lines represent the C2H2 zinc fingers domains. B. Percentage of eGFP cells obtained by FACS analysis on Tg(*BRE:eGFP*) fish.

Table S1. Sequence of primers used in this article (5'-3').

bif1-F	GGAAGAACCCTGCAGAATCCA
bif1-R	TCACATCAGCGTGAACAGGAA
bmp2b-F	GAAGAGGCTTTCGAGGCACT
bmp2b-R	CGTACTCGTCCAGGTACAGC
bmp7-F	CTTGTGGTTGCAGTGTGCTC
bmp7-R	TTTGTGCGGTGATGACCCTT
smad6a-F	GTATGTTCAGGACGAGACGCACG
smad6a-R	TTATCTGTGGTTGTTGAGTAAA
smad6b-F	GTATGTTCAGGACGAGAC
smad6b-R	TTATCTGTGGTTGTTGAG
smad7-F	AGGTGCTTTTACAGGCGGTT
smad7-R	CTTTATGCACCAGCAGCGTC
smad5-F	TGCGAGTATCCATTCGGCTC
smad5-R	TTGTCTGTGGTACTCGGCAC
smad9-F	ATGCTTCCCTCCACAACGAG
smad9-R	CCGTGGTTTACCGACTGTGA
bmp1b-F	GCGTGCTGGTGCTCATTTTT
bmp1b-R	CGAGCGAGTCCACATCATCT
tolloid-F	CAACTCTCTTGGTGAGCCGT
tolloid-R	CGACCAATCAGAGGGCTGTT
bmpr1ab-F	AGGAGAAAATGTGGCGGTGA
bmpr1ab-R	AAGCACTCGTCACTGTTCCA
bmpr1ba-F	TGGCTCAGGACTCCCTCTAC
bmpr1ba-R	TTGGGGAAGGAGGGTCGTAT
bmpr2b-F	TCCAAATCTTCATCTGCACTAACG
bmpr2b-R	CTCGCCCATCATCACACGAT
Full length primers	
bif1-FL-F	CAGAATTCGCATGGAGACTGAGGAAGAACC
bif1-FL-R	AATCTAGAACAGGGCTAATTCTTTCCTCC
bmp2b-FL-F	CAGAATTCGCAACTGACTGATCATGGTCGC
bmp2b-FL-R	AATCTAGAAGGAGATTGTTCTCATCGGCA
smad6a-FL-F	AACGGATCCTCGTATGTTCAGGACGAGACGCACG
smad6a-FL-R	AAACTCGAGGGTTATCTGTGGTTGTTGAGTAAA
Cloning primers	
bif1- promoter-F	GCCCGCGGCCCATACTTCACAGTTGGGA
bif1- promoter-R	GCGCGGCCGCTCTCCTGCTGTAATTCCTCC
bif1- codingsequence-F	AAGGATCCACCATGGAGACTGAGGAAGAACC
bif1- codingsequence-R	CATCACTCTGGAGGAAAGAATAATCGATTA
qPCR primers	
bif1-qpcr-F	GGAGACTGAGGAAGAACCCTG
bif1-qpcr-R	TTTTTCTACACTTCGAGCAGCTG
ef1a-qpcr-F	GAGAAGTTCGAGAAGGAAGC
ef1a-qpcr-R	CGTAGTATTTGCTGGTCTCG
gata1-qpcr-F	TGAATGTGTGAATTGTGGTG
gata1-qpcr-R	ATTGCGTCTCCATAGTGTTG
Morpholino efficiency primers	
bif1-short-F	GGAAGAACCCTGCAGAATCCA
bif1-short-R	TTCCACACTGAGTGCATGTG
bif1-long-F	same as probe *bif1-FL-F*
bif1-long-R	same as probe *bif1-FL-R*

Table S2. Morpholino Sequence (5’-3’)

MO-control	CCTCTTACCTCAGTTACAATTTATA
MO-bif1	ATCCTCATCTGTGGAAAGATTAGGT